WYLE LABORATORIES
SCIENTIFIC SERVICES AND SYSTEMS GROUP
EASTERN OPERATIONS
FACILITIES LOCATED IN
HUNTSVILLE, ALA. AND HAMPTON, VA.

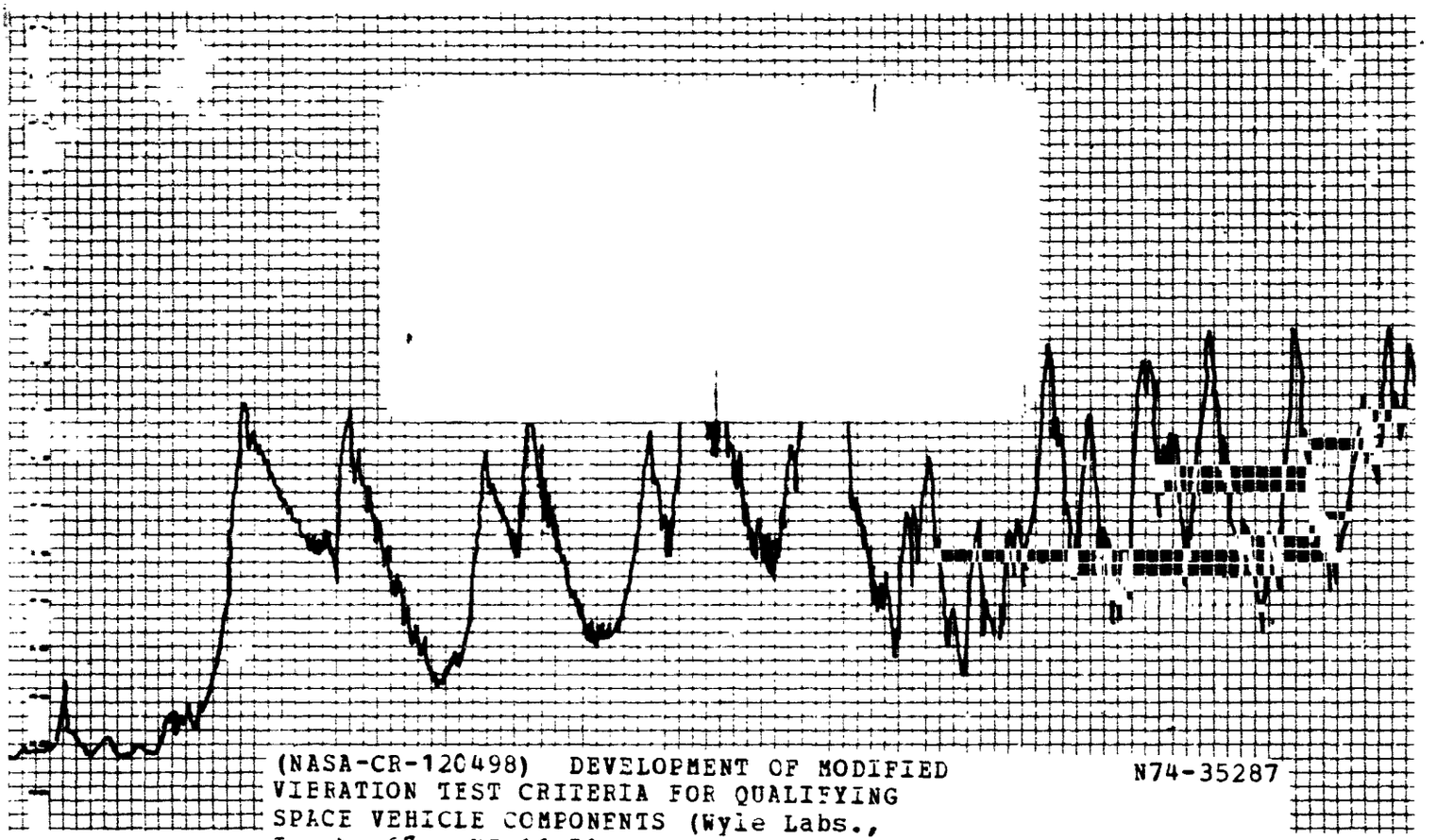

(NASA-CR-120498) DEVELOPMENT OF MODIFIED VIBRATION TEST CRITERIA FOR QUALIFYING SPACE VEHICLE COMPONENTS (Wyle Labs., Inc.) 67 p HC $6.50 CSCI 22B

N74-35287

Unclas
G3/31 52228

research REPORT

WYLE LABORATORIES — RESEARCH STAFF
REPORT WR 74-6

DEVELOPMENT OF MODIFIED VIBRATION TEST CRITERIA FOR QUALIFYING SPACE VEHICLE COMPONENTS

By

K. Y. Chang
G. C. Kao

Work Performed Under Contract NAS8-30630

October 1974

WYLE LABORATORIES
SCIENTIFIC SERVICES AND SYSTEMS GROUP
P O BOX 1008 • HUNTSVILLE, ALABAMA 35807
TWX (810) 726-2225 • TELEPHONE (205) 837-4411

COPY NO. 06

ABSTRACT

This report presents two simplified methods to estimate the test criteria of primary structures at component attachment points subjected to broadband random acoustic excitations. The current method utilizes a constant smeared component mass attenuation factor across the frequency range of interest. The newly developed method indicates that the attenuation factor is based on a frequency dependent ratio of the mechanical impedances of both the component and primary structures. These procedures to predict the structural responses are considered as the present state-of-the-art and will provide satisfactory prediction results. Example problems were used to illustrate the application procedures of these two methods and to compare the significant difference. It was found that the lower test criteria can be obtained by the impedance ratio method and this is due to the results of considering the effects of component/primary structure interaction.

FOREWORD

The work reported herein was supported by the National Aeronautics and Space Administration, Marshall Space Flight Center, under Contract No. NAS8-30630 during the period of March 12, 1974 through September 30, 1974. Technical monitoring of the program was provided by Mr. J. Herring of the Aeroelastic and Acoustic Response Branch, Structural Dynamics Division, System Dynamics Laboratory, Marshall Space Flight Center, Huntsville, Alabama. The Principal Investigator was Dr. Kung Y. Chang, Senior Research Specialist, Wyle Laboratories, Huntsville, Alabama.

The work performed consisted of the development and illustration of the impedance ratio concept. Efforts were also made to evaluate the impedance ratio concept and the constant mass attenuation method with structural example problems. The computation of input impedances of component and primary structure were based on nomograms and design charts developed under Contract No. NAS8-25811.

TABLE OF CONTENTS

LIST OF FIGURES

1.0 INTRODUCTION

Research in seeking practical techniques or methods for predicting vibration environments of space vehicles subjected to random acoustic pressure has gained considerable attention in recent years. As a result, several methods and techniques have been developed for dynamic environment predictions. Of these methods, Barrett (Reference 1) used a standardized approach to predict vibro-acoustic environments with sufficient conservatism to meet design and test requirements. This approach or so-called constant mass attenuation method is based upon the fact that similar structures have similar response characteristics but do not account for the component-primary structure coupling effects and the characteristics of frequency variations. However, it does provide a means to estimate the response of highly complex structures with only a few simple computations. Other methods such as described in References 2 and 3, utilize mechanical impedance concepts to predict broad frequency range vibration criteria. The impedance method was derived from a one-dimensional mathematical model and the prediction equation is expressed in terms of four types of parameters at component mounting locations. These parameters consist of input impedance of primary structure, input impedance of component package, acoustic mobility and blocked pressure spectrum. The predicted environments obtained from this method have been shown to be accurate and conservative within acceptable tolerance limits.

The objective of this report is to present the above two prediction methods and to compare their predicted results. A description of these methods is presented in Section 2.0. In Section 3.0, the approximate equations used to compute the four impedance parameters for the impedance prediction equation are described. The approximate equations were further converted into nomograms and computation charts and the resultants, and its application guidelines are given in Section 4.0. In Section 5.0, example problems are used to demonstrate the application procedures and to compare the difference of these two methods. Finally, a summary of the mechanical impedance method and the concluding remarks are described in Section 6.0. The development of the impedance prediction equations are described in detail in Appendices A, B and C.

2.0 METHODS FOR PREDICTING ENVIRONMENTS

2.1 Constant Mass Attenuation Method

The equation for predicting the vibration environment of acoustically susceptible structures is (Reference 1):

$$G_n = G_r \left(\frac{p_n}{p_r}\right)^2 \left(\frac{\rho_r h_r}{\rho_n h_n}\right)^2 F \qquad (2.1)$$

where:

G_n = the vibration response of the new vehicle structure at a particular location. The term G is the acceleration due to cyclic motion divided by the acceleration of gravity. Since rocket vehicle vibrations contain many frequencies the response magnitude (G) is specified in mean square spectral form.

G_r = the known vibration response of a reference vehicle structure. This value has been determined by measurements and is also presented on a spectral basis.

h_r = the thickness of the skin associated with G_r.

ρ_r = the skin weight density of the reference structure.

p_r = the impinging acoustic pressure which is driving the reference structure.

h_n = the skin thickness associated with G_n

ρ_n = the skin weight density associated with G_n

p_n = the acoustic pressures impinging upon the new vehicle structure. This pressure must be predicted.

F = a factor which accounts for the attenuation effects produced by incorporating additional mass into the existing system.

The above equation applies to random rms composite values or to sinusoidal values. The concept used to derive this equation is based on the assumption that similar structure exhibits similar dynamic characteristics. Once the frequency and amplitude characteristics of a typical type of structure have been adequately defined, these results may then be utilized as a basis for predicting the vibration environment of like structures.

The foregoing equation is applicable to localized vibratory environments and is valid for all materials. It is invalid when considering large sections of vehicle structure (i.e., entire cylindrical tank). However, the static loading of these large sections is the critical design factor and localized dynamics thereby produce only negligible effects.

In Equation (2.1), the expression indicates that for a constant driving power the structural response decreases as the weight density increases. For an item of component to be mounted on the structure in which the vibration environment has previously been defined, the vibration responses will be decreased by a factor of F. Therefore, the loaded response spectra, G_c, of the structure with component attached can be expressed as:

$$G_c = G_n \left(\frac{W_n}{W_n + W_c} \right) \tag{2.2}$$

where: W_n = effective weight of primary (support) structure.

W_c = component weight.

When determining the effective weight of structures, the radial distance should not exceed three times the distance between rings. This is because the dynamic characteristics of thin plates remain essentially constant above aspect ratios of three. In the preliminary development period, the weight of the basic structure or component may not be known and the attenuation factor is considered as unity. This will result in an estimate of the vibration environment which may tend to be conservative.

2.2 Impedance Ratio Method

The response prediction equation is derived based on a one-dimensional structural model. By applying Thevenins' and Norton's theorems to this model, the relationship between the unloaded and loaded response spectra is obtained and can be shown to have the following expression (References 2 and 3):

$$\Phi'_{\alpha}(\omega) = \Phi_{\alpha}(\omega) \cdot \left| \frac{Z_s(\omega)}{Z_s(\omega) + Z_L(\omega)} \right|^2 \tag{2.3}$$

where: $\Phi'_{\alpha}(\omega)$ = Power Spectral Density (PSD) of loaded response spectrum.

$\Phi_{\alpha}(\omega)$ = PSD of unloaded structural response spectrum.

$Z_s(\omega)$ = Input impedance of primary support structures.

$Z_L(\omega)$ = Input impedance of component package.

ω = Frequency parameter.

An analytical approach to compute the unloaded response spectrum has been established (Reference 4), and the equation is given as follows:

$$\Phi_{\alpha}(\omega) = \Phi_{p}(\omega) \cdot \left| \alpha(\omega) \right|^2 \qquad (2.4)$$

where: $\Phi_{p}(\omega)$ = Blocked sound pressure spectrum.

$\alpha(\omega)$ = Acoustic mobility of the structure.

The derivation of Equations (2.3) and (2.4) is presented in Appendix A. Equation (2.3) shows that the loaded response spectrum is equal to the response spectrum of the unloaded structure multiplied by the ratio of the impedances. The term $\left| Z_s(\omega) / Z_s(\omega) + Z_L(\omega) \right|$ serves as a magnification factor for both the unloaded and the corresponding loaded spectra and its value will approach unity when the structural impedance, $Z_s(\omega)$, becomes infinite. The impedances expressed in Equation (2.3) can be obtained directly from measurements on the actual structure. Nevertheless, all of the above quantities can be obtained through analytical prediction techniques. The equations and guidelines for predicting the input impedance and unloaded response spectra of structures are presented in the subsequent sections. The computation of the loaded response spectrum is illustrated by an example problem as described in Section 5.0 of this report. A flow chart indicating the computation sequence is shown in Figure 2.1.

3.0 IMPEDANCE DESIGN EQUATIONS

3.1 Prediction of Structural Impedances

Input impedances, $Z_L(\omega)$ and $Z_s(\omega)$, in the impedance ratio equation are specified in terms of the "force/velocity" format. Input impedance of component package, $Z_p(\omega)$, is defined as an ideal damping, spring and mass system, and is described in Appendix B. The primary support structures considered herein consist of basic cylindrical shells, longitudinal stringers and ring frames. The cylindrical shells are stiffened by stringers in the axial direction, and ring frames are attached inside the shell wall. The direction of vibratory response under consideration is referred to as that normal to the skin which is excited by impinging acoustic pressures. The stiffeners are not directly excited by acoustic forces but are driven by the motion of adjacent panels. The approximate equations for predicting the input impedance of these three structural components have been reported in detail in Reference 4 and are briefly summarized in Appendix C. For the sake of completion in the presentation, this report encompasses all the pertinent equations from the reference necessary to compute the input impedance of structures. The approximate equations are given in Table 3.1 in three different frequency ranges as defined below (Reference 5):

- Low frequency range or frequencies below the fundamental frequency of the shell,
- Intermediate frequency range, and
- High frequency range or frequencies above the ring frequency of the shell.

The evaluation of the stiffened shell impedances, $Z_s(\omega)$, is then obtained for the above three frequency ranges as follows:

Low Frequency Impedances — The static stiffness is the predominant factor which influences the input impedance. Due to the lack of theoretical expressions for input impedances of stiffened cylindrical shells, it is assumed that at low frequencies the input impedance at any location follows the stiffness line, this stiffness being equal to the summation of the stiffness of the individual structural elements that are present in that location. Two cases are considered in this frequency range, namely:

- If the stiffness of the ring is small in comparison to the stiffness of the stringer or the unstiffened shell, the overall stiffness can be computed by adding the stiffness of the properly modeled structural elements that are present at the input location, as follows:

$$K = K_s + \sum K_B + \sum K_R \tag{3.1}$$

where:

K_s = static stiffness of shells

K_B = static stiffness of beams or stringers

K_R = static stiffness of rings

Thus the input impedance of a stiffened cylindrical shell at low frequency follows a stiffness line whose value can be computed from the sum of stiffnesses of structural elements at that point.

- For a stiffened cylindrical shell, if rings are sufficiently stiff in comparison with the entire shell, these rings act like the boundary of structure panels. Then the characteristic impedance of the shell can be determined from the length of the spacing between two adjacent rings.

$$K = K_s + \sum K_B \tag{3.2}$$

The characteristic impedance represents the impedance of a str[illegible] of such a length that reflections from the boundaries are negligible. In other words, the resonance modes of a structure with any non-dissipative boundary conditions are identical to the resonance modes of a supported structure whose length is equal to the distance between the node lines.

Intermediate Frequency Impedances — Within the intermediate frequency range, which extends from the fundamental frequency to the ring frequency, the input impedances of the test specimens can be evaluated as the combination of the characteristic impedances of the primary structural components. The equation is written as:

$$Z = Z_s + \sum Z_B + \sum Z_R \tag{3.3}$$

where:

Z_s = characteristic impedance of shells

Z_B = characteristic impedance of stringers

Z_R = characteristic impedance of rings

High Frequency Impedances — The input impedance of a stiffened shell at high frequencies depends on the location of a measurement point and is evaluated by the following rules:

- Unstiffened (skin) Point — The input impedance approaches that of an infinite plate of the same thickness.
- Stiffened Point — The skin and the stiffener(s) decouple dynamically at high frequencies, therefore, the input impedance approaches that of the stiffener(s).
- Stiffened Intersection Point — The input impedance at the centers of short stiffeners segments are generally higher than those of longer stiffener segments; and the impedance at an intersection of the stiffeners is approximately equal to the sum of the individual impedances of the two stiffeners — the ring impedance and stringer impedance.

3.2 Prediction of Acoustic Mobility

Acoustic mobility, $\alpha(\omega)$, is defined as the ratio of the mean-square spectral density of the velocity to the mean-square spectral density of the fluctuating pressure driving the structure. This quantity is expressed by Equation (3.4) as follows:

$$\alpha(\omega) = \frac{S_{\dot{u}}(\omega)}{S_p(\omega)} \tag{3.4}$$

where $S_{\dot{u}}(\omega)$ has units of $(\text{in./sec})^2/\text{Hz}$, and $S_p(\omega)$ is the blocked pressure spectral density having units of $(\text{psi})^2/\text{Hz}$. The blocked pressure includes the effects of reflection and thus accounts for the pressure doubling effect when an object is immersed in a random pressure field.

Generally, the acoustic mobility for a given structure would be calculated based upon modal analysis or statistical energy analysis. However, for the purposes of presenting simplified design techniques, empirical curves may be used for defining acoustic mobility. The development of these empirical curves from a broad range of available vibro-acoustic data is described in detail in Appendix C of Reference 4. Only the main results will be presented in this report. The basic design curves for acoustic mobility are shown in Figure 3.1 for two values of damping: $Q = 20$ and $Q = 200$. In this figure, the normalized acoustic mobility derived from the measurements is expressed as:

$$\alpha'(\omega) = \frac{S_{\dot{u}}}{S_p}\left(\frac{m}{D}\right)^2 \tag{3.5}$$

and has units of $(\text{in./sec})^2/\text{in.}^2$ The abscissa of this figure is fD, i.e., frequency times cylinder diameter in units of Hz - in.

In order to use the empirical curves of Figure 3.1, an estimate of the structural damping, Q, must first be obtained. Then by stustituting for vehicle diameter, D, and surface weight, m, the acoustic mobility $S_{\dot{u}}/S_p$ (or α) may be determined as a function of frequency, f Hz. For structural Q values other than those shown in Figure 3.1, the acoustic mobility term may be interpolated since an increase in Q by a factor of 10 results in an increase in the acoustic mobility term of one decade.

3.3 Evaluation of Blocked Pressure

The blocked pressure spectrum, $\Phi_p(\omega)$, is defined as the effective acoustic pressure acting on a primary structure. The pressure is equivalent to that acting on a rigid cylinder which has the identical geometrical dimensions as the primary structure. This pressure can be determined from the far-field sound pressure measurement and is given by (References 6 and 7):

$$\mathcal{J} = \frac{\left[P^2_{block} \right]}{\left[P^2_{far} \right]} = 4\,(\pi k R)^{-2} \sum_{m=0}^{\infty} \epsilon_m \left| H'_m (kR) \right|^{-2} \qquad (3.6)$$

where:

$\left[P_{far} \right]$ = measured sound pressure levels without the presence of flexible structures

k = wave = $2\pi f/c$

c = speed of sound in acoustic medium; for air $c = 13{,}400$ in./sec

R = radius of cylinder = $D/2$

ϵ_m = Neumann factor = 1 for $m = 0$, 2 for $m > 0$

$H'_m(kR)$ = derivative of Hankel function of order, m

The foregoing equation is derived from an infinite panel and does not account for diffraction effects of structures with finite length. However, the error due to diffraction effects is considered as insignificant and will not influence the final results. In the frequency range of interest, the rms blocked sound pressure is approximately 40 percent higher than the measured sound pressure and such a conversion factor generally leads to conservative estimates of the force spectra.

The curve representing the expression of Equation (3.6) versus fD is shown in Figure 3.2 and can be used to evaluate the blocked pressure spectra on the surface of cylinders in a reverberant acoustic environment.

4.0 COMPUTATION CHARTS AND GUIDELINES

In order to minimize manual efforts in performing response computations, it is necessary to reduce the derived equations described in Section 3.0 into the form of nomograms or charts so that lengthly computations can be avoided.

All equations in Table 3.1 contain a frequency dependent and a frequency independent terms. Therefore, by evaluating the frequency independent term, and later, combining with the frequency dependent term, the impedance curve can be easily constructed. The approaches, which are based on the separation of the frequency dependency to simplify the impedance prediction, are presented below.

4.1 Nomographic Charts

A nomograph, in its simplest and most common form, is a chart on which one can draw a straight line that will intersect three or more scales in values that satisfy an equation or a given set of conditions. The equations summarized in Table 3.1 were converted into nomographic forms, and are shown in Figures 4.1 through 4.6. Figure 4.1 evaluates the static stiffness of the ring frame. By knowing the values of radius, R, and the flexibility, EI, of the ring, and connecting these two values on the R scale and the EI scale with a straight line, the intersection point in the K scale represents the computational result of the given equation.

Figures 4.2 and 4.3 perform similar computations for static stiffness of beams and the frequency independent part of beams and ring frames which is defined as:

$$Z_r = 2\sqrt{2}\,\rho A \left[\frac{EI}{\rho A}\right]^{1/4} \tag{4.1}$$

Figure 4.4 is a four-variable type nomogram for evaluating static stiffness of unstiffened cylinders. By using one additional axis, T, which lies between the ℓ and R axes and need not be graduated, the equation was broken into two three-variable equations and are handled as the preceding way, i.e., connecting the ℓ scale and the R scale with a straight line, then joining the intersection point on the T axis and the h scales with another straight line, the intersection point on the K scale is the resulting value.

Figure 4.5 is used to evaluate the frequency independent part of the shell impedance as defined below:

$$Z_f = \frac{4}{\sqrt{3}}\,\rho h^2 \sqrt{\frac{E}{\rho R}} \left(\frac{E}{\rho}\right)^{1/4} \tag{4.2}$$

Figure 4.6 is used to evaluate the infinite plate impedance, Z_p, according to the expression shown in Table 3.1.

4.2 Charts for Computing Structural Impedance

The impedance of an ideal damping, spring and mass system may be represented by three intersection lines. By using this approach, the driving-point impedance for beams and rings based on the equations of Table 3.1 were represented by two sets of intersection lines varying with the frequency as shown in Figure 4.7. In this figure, the line representing the proper stiffness value is obtained either from the result of Figure 4.1 or 4.2 for rings and beams, respectively, and the line defining the proper Z_r value of the structure is determined from Figure 4.3. The stiffness lines represent the impredance at low frequencies and the Z_r lines represent the impedance at high frequencies. The intersection of these two lines determines the fundamental resonant frequency of the structural system. In this figure and the following figures, a scale factor is used to obtain correct scale values for the standard diagrams.

The driving-point impedance for unstiffened cylindrical shells is shown in Figure 4.8, where the Z_r lines are replaced by the Z_f lines. The lines represented the proper stiffness, Z_f and infinite-plate impedance are obtained from Figures 4.4, 4.5 and 4.6, respectively. At low frequencies, the impedance of cylinders follows a stiffness line and at high frequencies the impedance is equal to the impedance of an infinite plate which has a constant value. Within the intermediate frequency range, the input impedance may be represented by the Z_f line.

The fundamental frequency and the ring frequency of cylinders are determined by the intersection of these three characteristic lines.

The impedance of the stiffened cylinder is equal to the linear summation of these component curves and is obtained in the following manner:

- The logarithmic summation chart (LSC) shown on the upper portion of these charts will be used to compute the linear summation of two impedance curves.
- At any frequency point, measure the difference of two impedance values and use this length as the abscissas value in the LSC.
- The ordinate corresponding to the abscissas in the LSC is the resulting value for these two curves in logarithmic summation.
- Add the length of the ordinate to the upper impedance curve, the resulting curve denotes the linear combination of these two impedances.

Figure 4.9 represents the impedance lines for the component package which are defined as an ideal damping, spring and mass system. The graph shown on the upper portion of this computational chart will be used to compute the logarithmic ratio of two impedance curves. The application of the LSC is similar to the procedure as described before except that the length of the ordinate obtained from the LSC is subtracted from the lower impedance curve. The usage of the LSC is demonstrated in Section 5.0.

4.3 Charts for Computing Blocked Pressure

The conversion of a far-field sound pressure spectrum into a corresponding blocked pressure spectrum is achieved by multiplying the far-field pressure spectrum by the correction coefficient, 3 , as shown in Figure 3.2. To obtain the $\sqrt{3}$ -coefficient for a particular cylinder in the frequency scale, it is accomplished by shifting the fD scale in Figure 3.2 to the left for the amount corresponding to the cylinder diameter, D. For example, if the diameter of a cylinder is 48 inches, the $\sqrt{3}$ -coefficient for that cylinder is obtained by shifting the fD scale by a factor of 48 to the left, as shown by the $\sqrt{3}$ -curve in Figure 4.10. The blocked pressure spectrum of the far-field pressure spectrum is then obtained by adding the $\sqrt{3}$ length values at each frequency point to the far-field sound pressure.

4.4 Charts for Computing Response Spectrum

The unloaded response spectrum is obtained by the product of the blocked pressure spectrum obtained from Figure 4.10, and the velocity acoustic mobility. The normalized acoustic mobility curves as shown in Figure 3.1 must be converted to $|\alpha^2|$ versus frequency format for use in response computation. The conversion can be accomplished graphically by shifting the abscissas scale to the left corresponding to the diameter of a cylinder, D; and shifting the ordinate scale upward or downward corresponding to the quantity $(m/D)^2$. For example, by applying the above procedures to an aluminum cylinder with D = 48 inches, Q = 20, and $(m/D)^2 = 3.34 \times 10^{-8}$ lb/in.^{3}, the acoustic mobility for the cylinder is obtained and is shown in Figure 4.11. The unloaded velocity response spectrum is obtained by summing up logarithmically the velocity acoustic mobility curve and the blocked pressure spectrum as explained in Figure 4.11.

The impedance ratio and the unloaded response spectrum obtained from Figures 4.9 and 4.11, respectively, are again plotted on a new computation chart for final computation. This chart has the same form as Figure 4.11. At any frequency point the sum of these two curves shown on the chart is the resulting loaded response spectrum for the design structural system.

Note that all charts developed in this section are in same length scale and the transfer of data curves from one chart to the next chart can be easily done by overlay technique. Example problems to illustrate this simplified technique to predict vibratory environments for space vehicles are explained in detail in the following section.

5.0 EXAMPLE PROBLEMS FOR COMPARISON

To aid in understanding the computation procedures and to compare the results of these two prediction methods described in Section 2.0, example problems are illustrated in this section. The specimen used in the prediction consists of a basic cylindrical shell, four longitudinal stringers and two circumferential ring frames. The basic cylindrical shell has overall dimensions of 96.0 in. (length) x 48.0 in. (diameter) x 0.08 in. (thickness). All structural elements were made of aluminum. The ring frames are built-up channel sections which are attached to the inside surface of the shell wall by means of rivets; and, the stringers are angle sections which are similarly attached to the outside surface of the shell wall. The dimensions of the curved panels formed by the stiffeners were 32.0 inches and 37.7 inches. Two heavy end rings consisting of angle sections were welded to the inside surface at the two ends of the shell wall; and, thick circular plywood bulkheads were bolted to the end rings, and are used to provide radial constraint at the ends of the shell wall. Its structural configuration is shown in Figure 5.1. Overall dimensions of the cylindrical structure are listed in Table 5.1. Details of structural configuration and corresponding test results can be found in Reference 5.

The computations of static stiffness, Z_r and Z_f for the primary structure components have been evaluated previously as shown in Figures 4.1 through 4.6. The impedance computations for the configuration with two ring frames and four stringers are illustrated in Figures 5.2 and 5.3. In the computation, it was assumed that these two rings act like end bulkheads with high structural rigidity so that the effective length of cylinder becomes the length of the middle segment which is equal to 32 inches. In Figure 5.2, the impedance for one stringer and four stringers are plotted based on the values obtained from Figures 4.2 and 4.3. Similarly, the impedance curve representing the unstiffened cylindrical shell is plotted in Figure 5.3, in which the impedance representing the sum of four stringers is also shown, except that at high frequencies where the structural system decouples dynamically and the impedance approaches that of one stiffener only. In Figures 5.2 and 5.3, the plotting scale is 10 times the correct value as indicated by Factor = 0.1. Based on the procedure of the LSC as described in Section 4.2, the impedance of the stiffened shell which is equal to the linear summation of these two component impedances is obtained and is also shown in Figure 5.3. Figure 5.4 shows the measured impedance data from Reference 5 along with the computed impedance for comparison. Generally speaking, the comparison is considered quite satisfactory both in low frequency and high frequency ranges. Fair agreement is also observed for frequencies just below the ring frequency. Some discrepancies are observed in the intermediate frequency region. Such discrepancies are attributed to the errors incurred in summing the impedances of the stringers. Further refinements in predicting techniques to achieve a higher degree of accuracy in this frequency range are needed. However, it may be concluded that the equations and guidelines outlined in Section 3.0 are adequate for determining the structural impedances for design purposes.

The simulated component package consisted of a 1/2 inch aluminum plate with lateral dimensions of 8.0 in. x 8.0 in. The plate was supported by four sets of leaf springs at its corners. The bottom of each spring was fitted with a load washer assembly. The total weight of the component package was 3.81 pounds; the resonances of the package were measured at

110 Hz and 1200 Hz, respectively. The latter frequency is the fundamental resonance of the 1/2 inch plate. Detailed descriptions of the structural configurations can be found in Reference 3.

The impedance of the component package was estimated and is presented in Figure 5.5 The predicted impedance for the stiffened cylinder is also shown in the same figure. These two impedance curves are combined to form the combined impedance curve according to the procedure as described in Section 4.2. The curve shown on the bottom of Figure 5.5 represents the length difference between the component impedance and the combined impedance at any frequency point. The resulting curve given is the impedance ratio term in the computation of the loaded response spectrum.

The blocked sound pressure and the acoustic mobility shown in Figures 4.10 and 4.11, respectively, were adopted to this example problem and the unloaded response spectrum is the vector sum of these two curves, and is also shown in Figure 4.11.

Based on the impedance ratio shown in Figure 5.5, the unloaded response spectrum of Figure 4.11 is converted into the loaded response spectrum, i.e., by summing these two individual curves. The final computation was performed on Figure 5.6, and the resulting test criteria is shown by the dashed line.

As discussed previously, the loaded response spectrum for this example problem can be obtained by the constant mass attenuation method. The equation for predicting the loaded response environment, G_c, of a component on the cylindrical structure is described in Section 2.1. Thus:

$$G_c = G_n \left(\frac{W_n}{W_n + W_c} \right) \tag{5.1}$$

in which these parameters were obtained as follows:

$$W_n = 0.1 \times (32 \times 37.7 \times 0.08) = 9.65 \text{ (lb)}$$

$$W_c = 3.81 \text{ (lb)}$$

Substituting the calculated values into Equation (5.1) results in:

$$G_c = 0.72\, G_n \tag{5.2}$$

Now, the resultant response environments, G_c, can be obtained by multiplying the ratio, as indicated by 0.72, by the unloaded response spectrum of Figure 4.11. Results of this computation along with the predicted response spectrum obtained by the impedance ratio method are presented in Figure 5.7. Note that this figure can also be used as the conversion chart to convert the acceleration PSD into velocity PSD and vice versa. The velocity response is read-off from the vertical scale of the left-hand side and the acceleration response is read-off from the right-hand side. As can be seen from this figure, predicted response obtained from the constant mass attenuation method is much too high in the intermediate frequency range (40 ~ 400 Hz), i.e., the vibration criteria established by this method, which ignores effects of component/primary structure coupling may provide too much conservatism to satisfy design and test requirements and there is a strong possibility that the specimen would be over-tested under such criteria. This method is valid only when the impedance of a primary structure is sufficiently higher than that of the attached component.

6.0 SUMMARY AND CONCLUSIONS

Two simplified methods were used to predict the loaded response spectrum of a component and its support structure (space vehicle) which is subjected to broadband random acoustic excitations. The newly developed method was derived from a one-dimensional impedance model and the computation is performed by way of nomograms and design charts. These techniques presented herein are considered indicative of the present state-of-the-art and will permit satisfactory environmental estimates of highly complex requirements with minimum amount of manual computations. However, the lower test criteria can be obtained by the impedance ratio method and this is due to the results of considering the effects of component/primary structure interaction.

A summary of the computation procedures of the impedance ratio method is presented below in outline form for quick reference.

STEP 1: Determine and compute the geometrical and material properties of cylinders and their components.

STEP 2: Evaluate the parameters of structural impedances of primary structural components, employing Figures 4.1 through 4.6. These impedances are summed in accordance with the guidelines described in Section 3.1 by using Figures 4.7 and 4.8.

STEP 3: Estimate the impedance of the component package and construct the component impedance curve by Figure 4.9. This curve is combined with the impedance curve obtained from Figure 4.8 to form the impedance ratio curve.

STEP 4: Determine the blocked pressure spectrum by means of the chart as shown in Figure 4.10. The unloaded response spectrum is computed by utilizing the chart as shown in Figure 4.11, or the response spectrum may be obtained from the experimental measured data.

STEP 5: Plot the unloaded response spectra and the structural impedance on the same chart. The loaded response spectrum for the design system is obtained by summing these two individual curves.

REFERENCES

1. Barrett, R. E., "Techniques for Predicting Localized Vibratory Environments of Rocket Vehicles," NASA TN D-1836, October 1963.

2. Kao, G.C., and Sutherland, L.C., "Development of Equivalent One-Dimensional Acoustic Force Spectra by Impedance Measurement Techniques," Wyle Laboratories Research Staff Report WR 69-11, May 1969.

3. Kao, G.C., "Prediction of Force Spectra by Mechanical Impedance and Acoustic Mobility Measurement Techniques," Wyle Laboratories Research Staff Report WR 71-16, October 1971.

4. Chang, K.Y., Cockburn, J.C., and Kao, G.C., "Prediction of Vibro-Acoustic Loading Criteria for Space Vehicle Components," Wyle Laboratories Research Staff Report WR 73-9, September 1973.

5. Conticelli, V.M., Kao, G.C., and White, R. W., "Experimental Evaluation of Input Impedances of Stiffened Cylindrical Shells," Wyle Laboratories Research Staff Report WR 70-12, August 1970.

6. Waterhouse, R. V., "Diffraction Effects in a Random Sound Field," JASA, Vol. 35, pp. 1610-1620, October 1963.

7. Conticelli, V.M., "Evaluation of Blocked Pressure Spectra on Stiffened Cylindrical Shells," Wyle Laboratories Research Staff Technical Memorandum, TM 71-1, September 1971.

TABLES

TABLE 3.1. SUMMARY OF INPUT-IMPEDANCE EQUATIONS OF BEAMS, RINGS AND SHELLS

Structure \ Frequency	Low Frequency Range $(f \le f_L)$	Fundamental Frequency, f_L	Intermediate Frequency Range $(f_L < f \le f_R)$	Ring Frequency, f_R	High Frequency Range $(f > f_R)$
Beam	$K_B = \frac{48\,EI}{\ell^3}$	$\frac{1}{2\pi}\left(\frac{\pi}{\ell}\right)^2 \sqrt{\frac{EI}{\rho A}}$	$Z_B = 2(1+i)\,\rho A \left[\frac{EI}{\rho A}\right]^{1/4} \sqrt{\omega}$		Same as Intermediate
Ring	$K_R = \frac{EI}{0.15R^3}$	$\frac{0.427}{R^2} \sqrt{\frac{EI}{\rho A}}$	$Z_R = i2\sqrt{2}\,\rho A \left[\frac{EI}{\rho A}\right]^{1/4} \sqrt{\omega}$		Same as Intermediate
Shell	$K_S = 2.5\,Eh \left(\frac{R}{L}\right)^{1/2} \left(\frac{h}{R}\right)^{1.25}$	$\frac{0.375}{L} \sqrt{\frac{Eh}{\rho R}}$	$\lvert Z_S \rvert = \frac{4}{\sqrt{3}}\,\rho h^2 \sqrt{\frac{E}{\rho R}} \left(\frac{E}{\rho}\right)^{1/4} \frac{1}{\sqrt{\omega}}$	$\frac{1}{2\pi R} \sqrt{\frac{E}{\rho}}$	$Z_S = \frac{4}{\sqrt{3}}\,h^2 \sqrt{E\rho}$
Stiffened Shell	$K = K_S + \Sigma K_B$ (or $+ \Sigma K_R$) $\lvert Z \rvert = K/\omega$		$Z = Z_S + \Sigma Z_B + \Sigma Z_R$		$Z = Z_S$, $Z = Z_B$, $Z = Z_R$

TABLE 5.1. SUMMARY OF DIMENSIONS, STIFFNESS AND MASS PROPERTIES OF CYLINDER AND ITS COMPONENTS

Property	Dimension	Structural Items		
		Ring	Stringer	Shell
Mean Radius, R	(in.)	23.0	---	24.0
Overall Length, ℓ	(in.)	144.5	96.0	96.0
Shell Skin Thickness, h	(in.)	---	---	0.08
Cross-section Area, A	($in.^2$)	.215	0.123	---
Moment of Inertia, I	($in.^4$)	.35	0.012	---
Weight per Unit Volume, ρ	($lb/in.^3$)	0.1	0.1	0.1
Modulus of Elasticity, E	($lb/in.^2$)	10^7	10^7	10^7
Weight per Stiffener *	(lb)	3.10	1.18	116.0
Total Weight of Structure	(lb)			126.92
Weight for Unit Surface	($lb/in.^2$)			8.7673×10^{-3}

* Two rings spaced at 32" in the longitudinal direction and eight longitudinal stringers spaced at 18.8" in the circumferential direction.

FIGURES

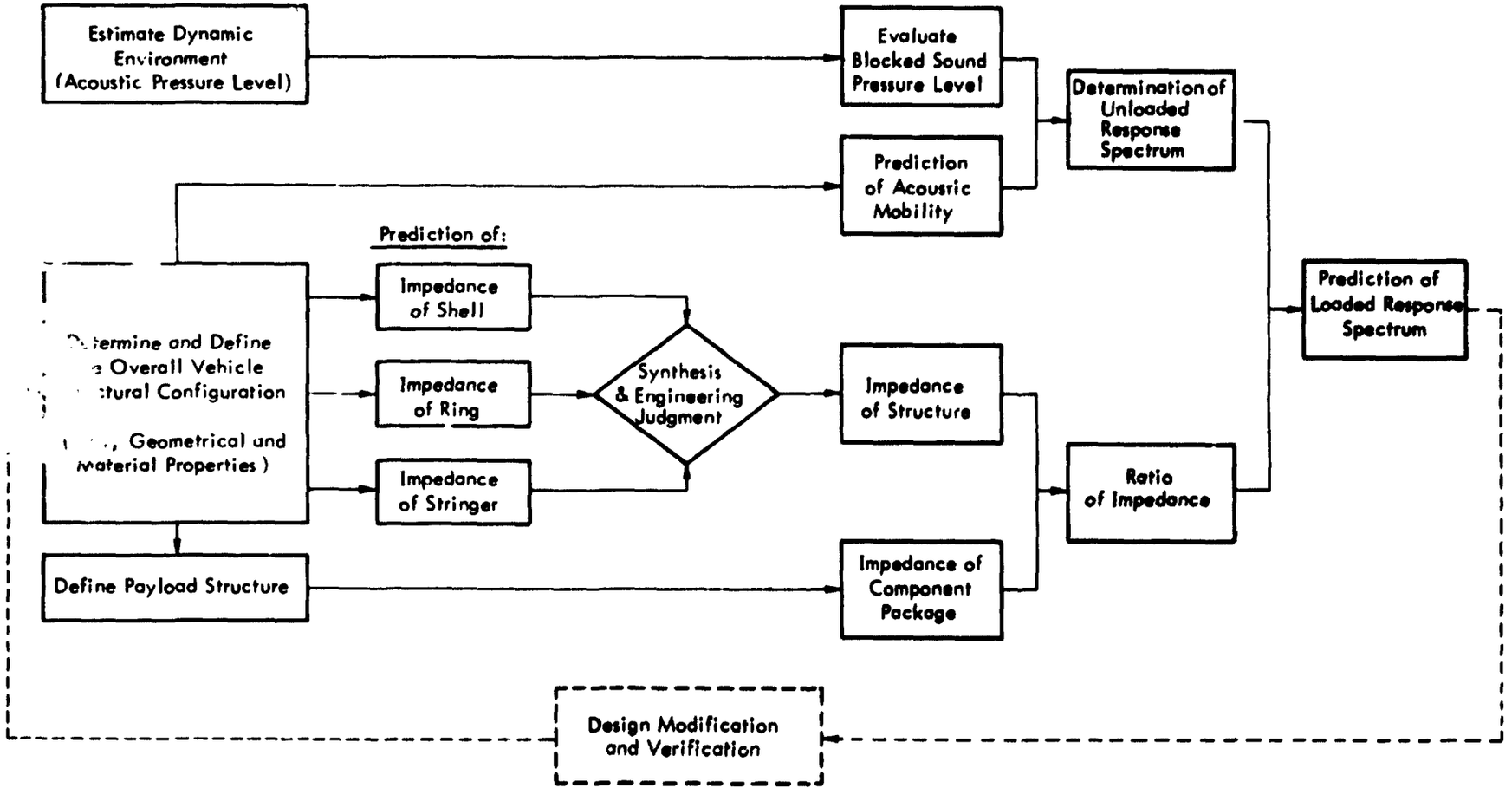

Figure 2.1. Flow Chart for Predicting the Loaded Response Spectrum of Structures

α = Acoustic mobility (in./sec/psi)

m = Surface density weight ($lb/in.^2$)

D = Diameter (in.)

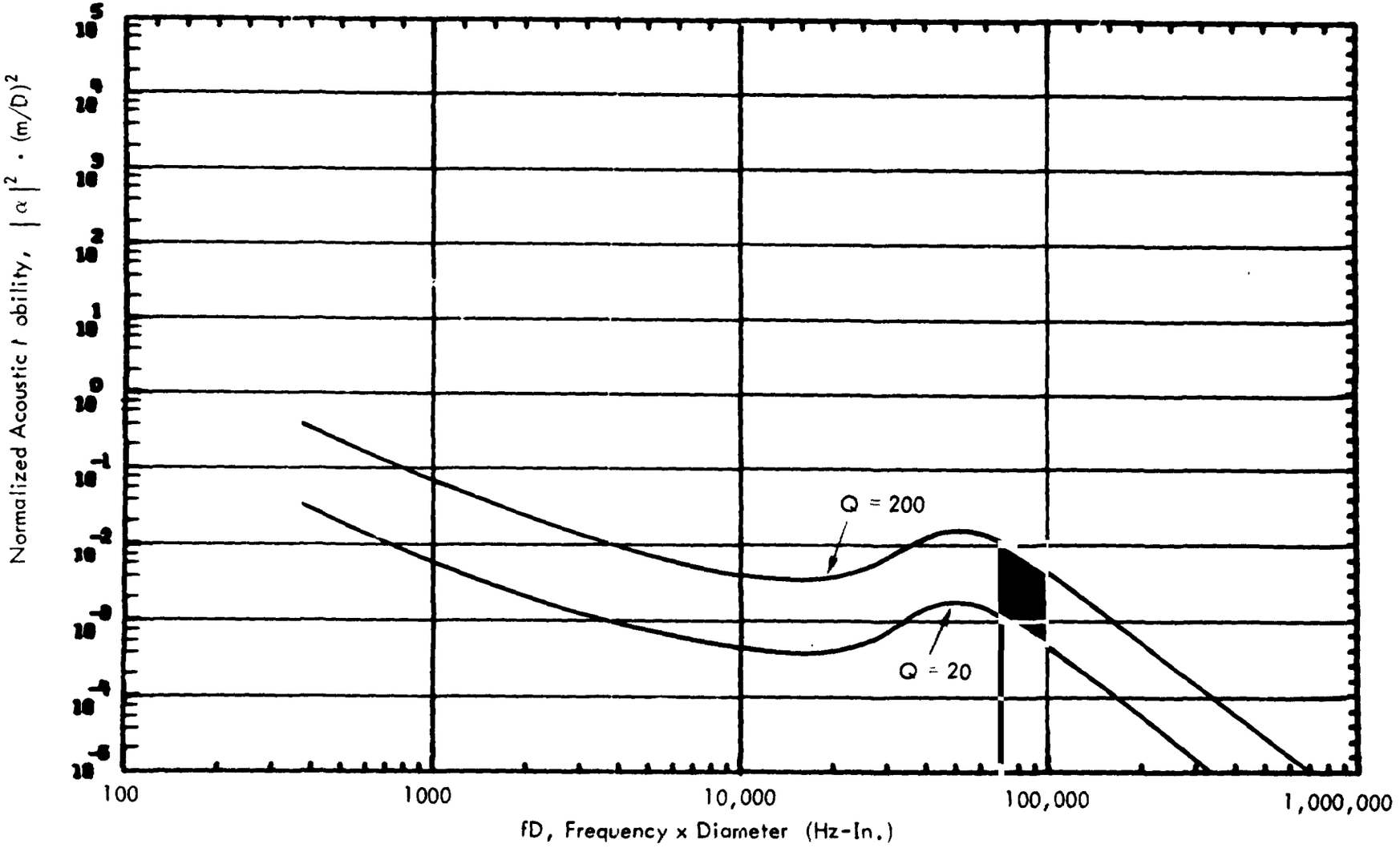

Figure 3.1. Velocity Acoustic Mobility Levels for Cylindrical Structures

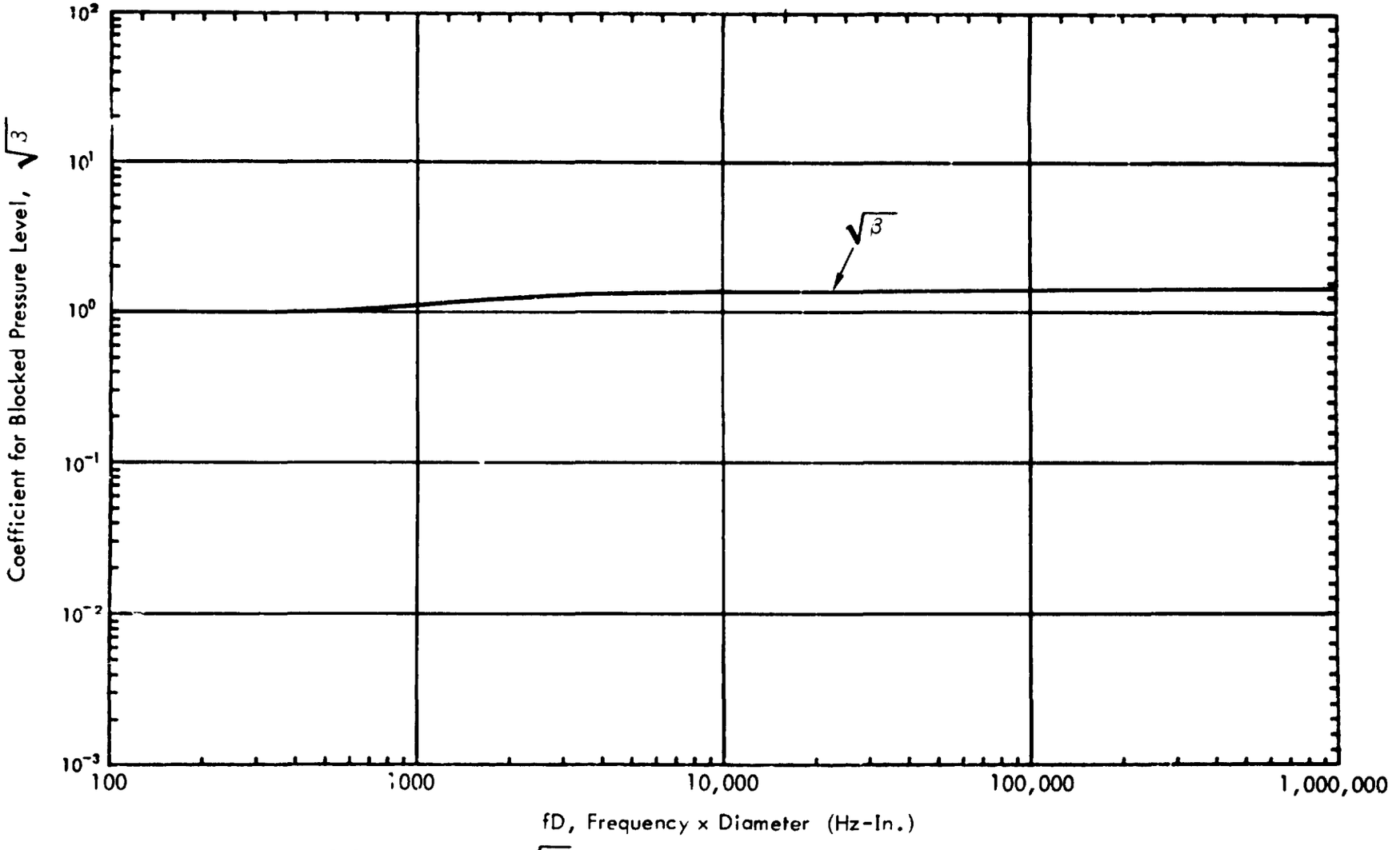

Figure 3.2. Theoretical $\sqrt{\beta}$ -Curve for Obtaining Blocked Pressure Level of a Cylinder in a Random Sound Field

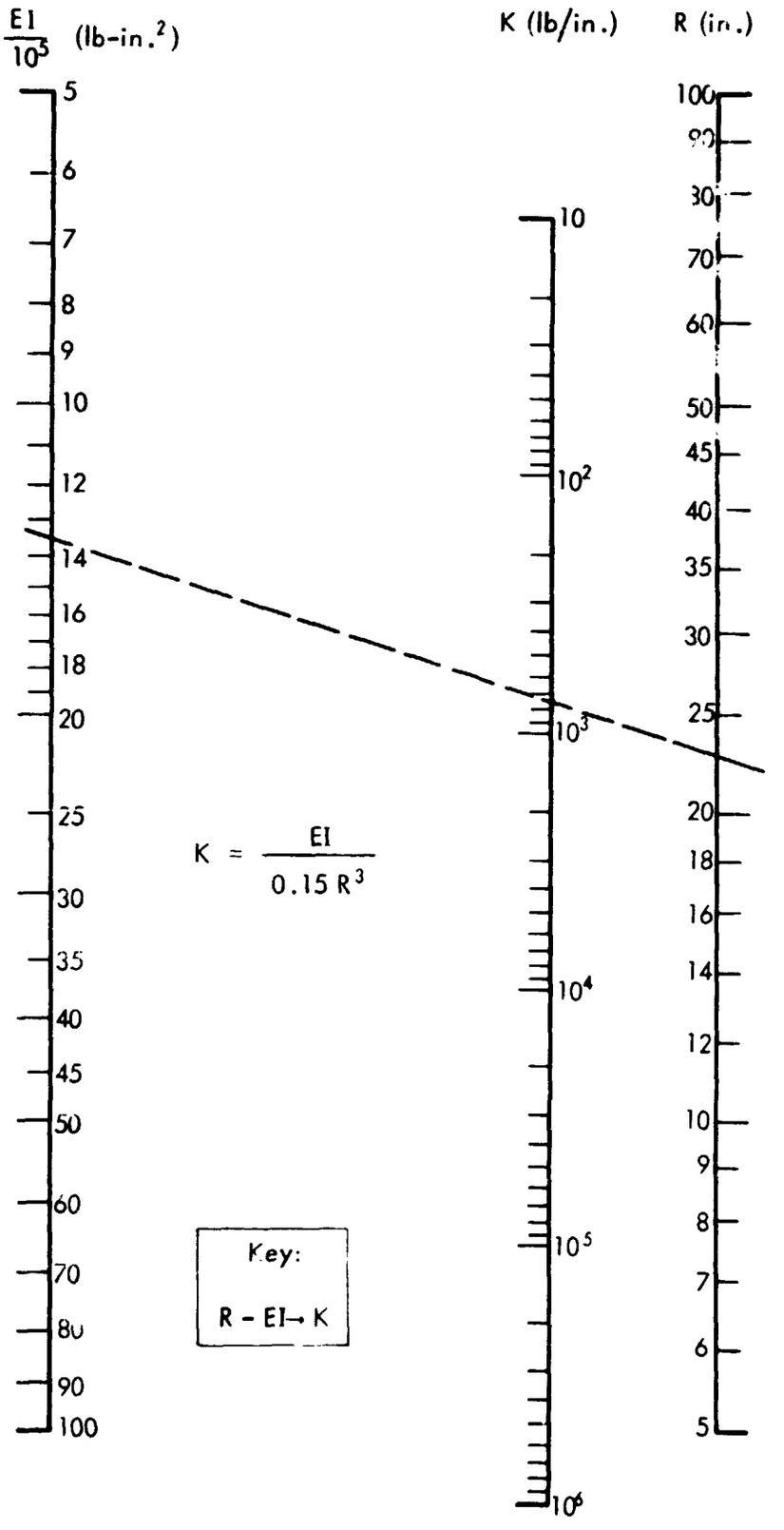

Figure 4.1. Nomograph for Determining Static Stiffness of Rings

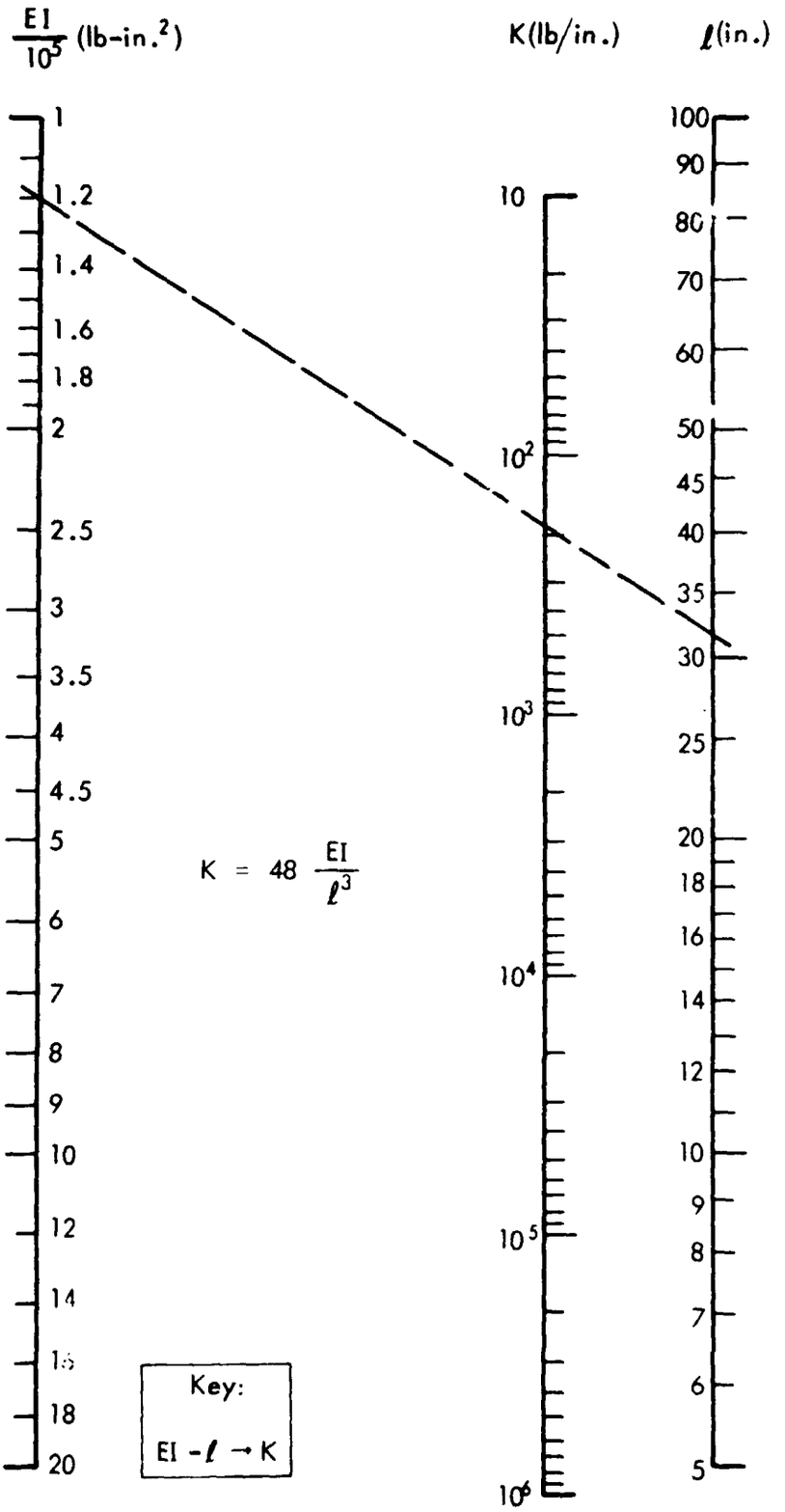

Figure 4.2. Nomograph for Determining Static Stiffness of Beams

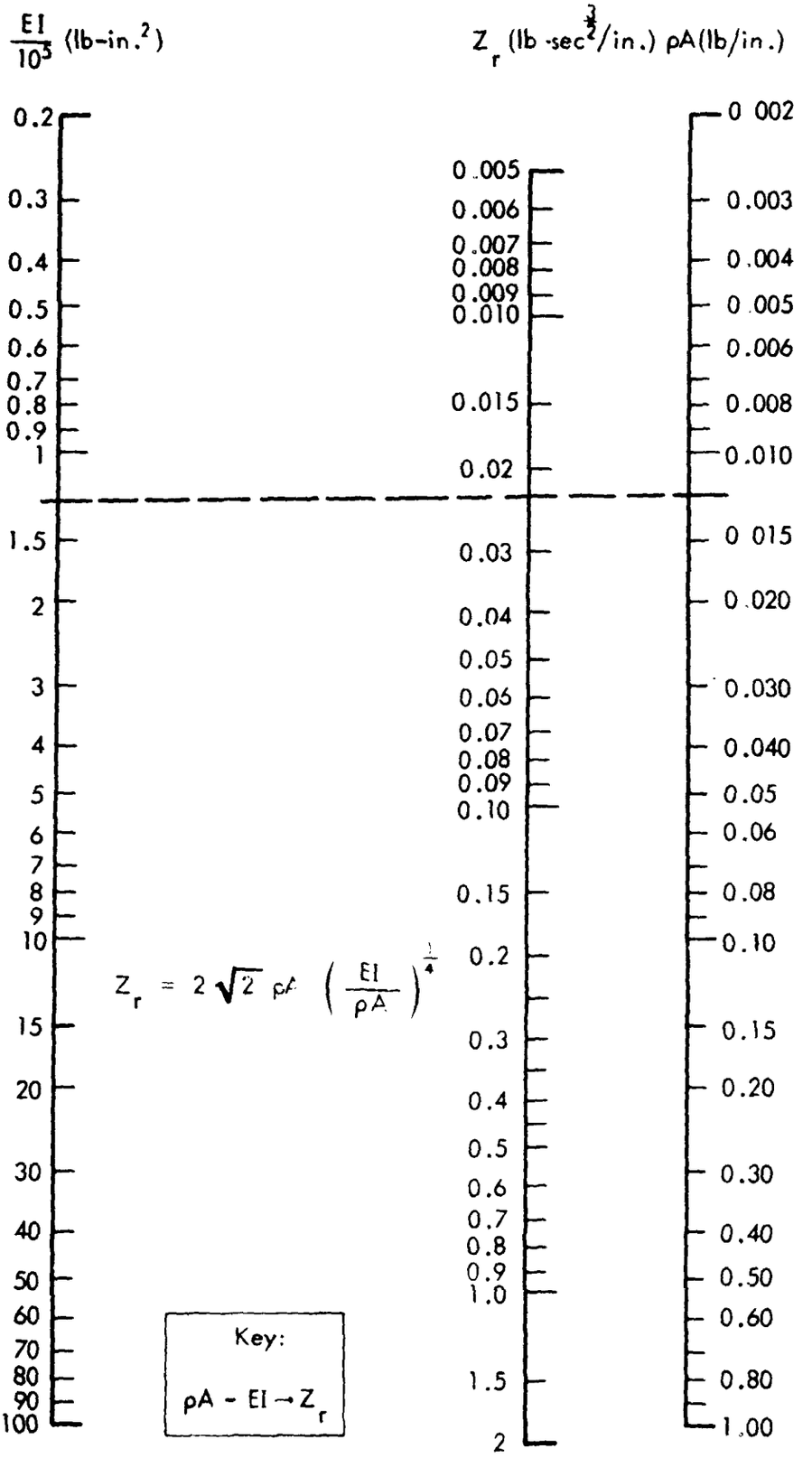

Figure 4.3. Nomograph for Determining Z_r of Beams and Rings

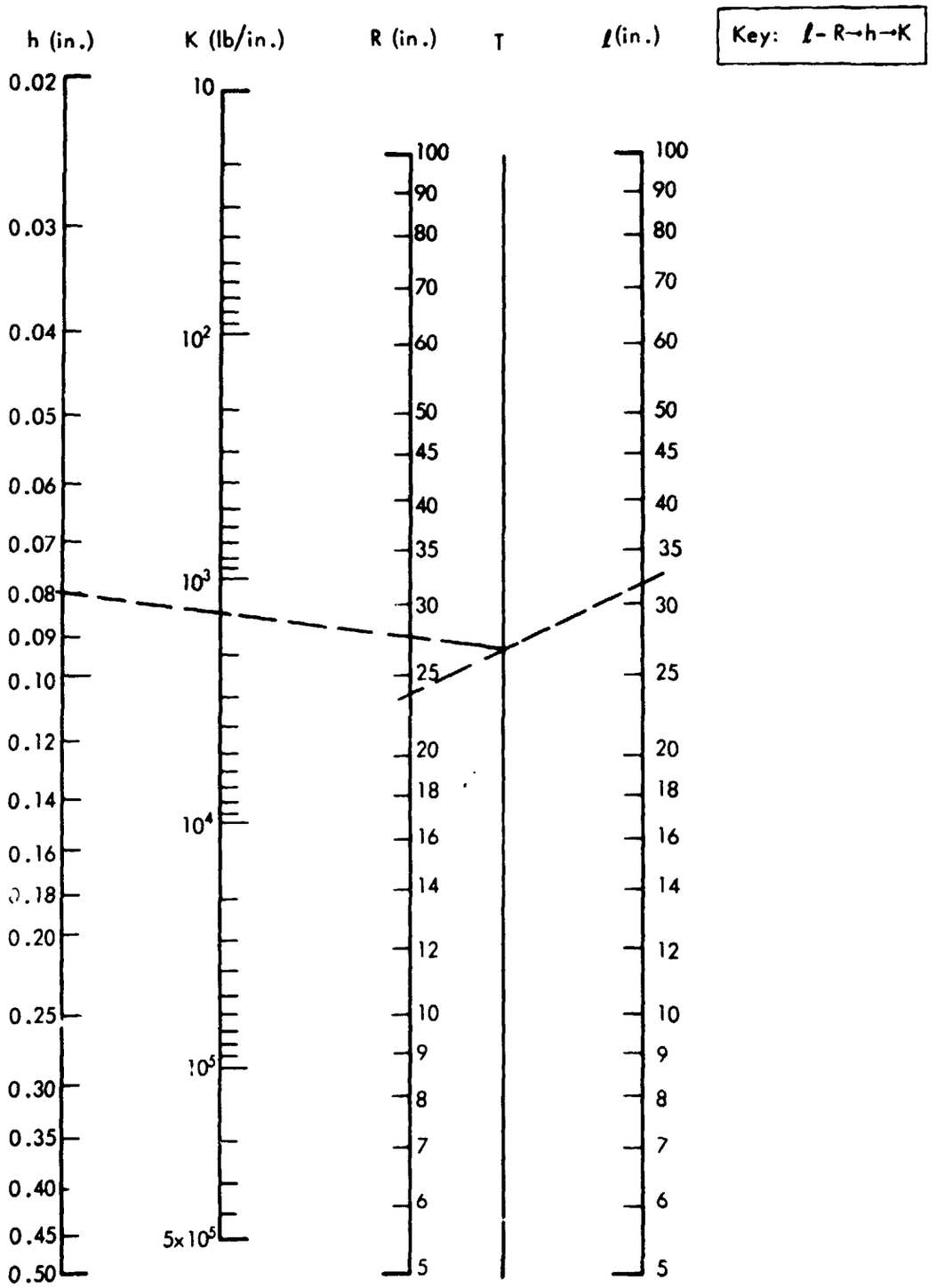

Figure 4.4 . Nomograph for Evaluating Static Stiftness of Unstiffened Cylinders

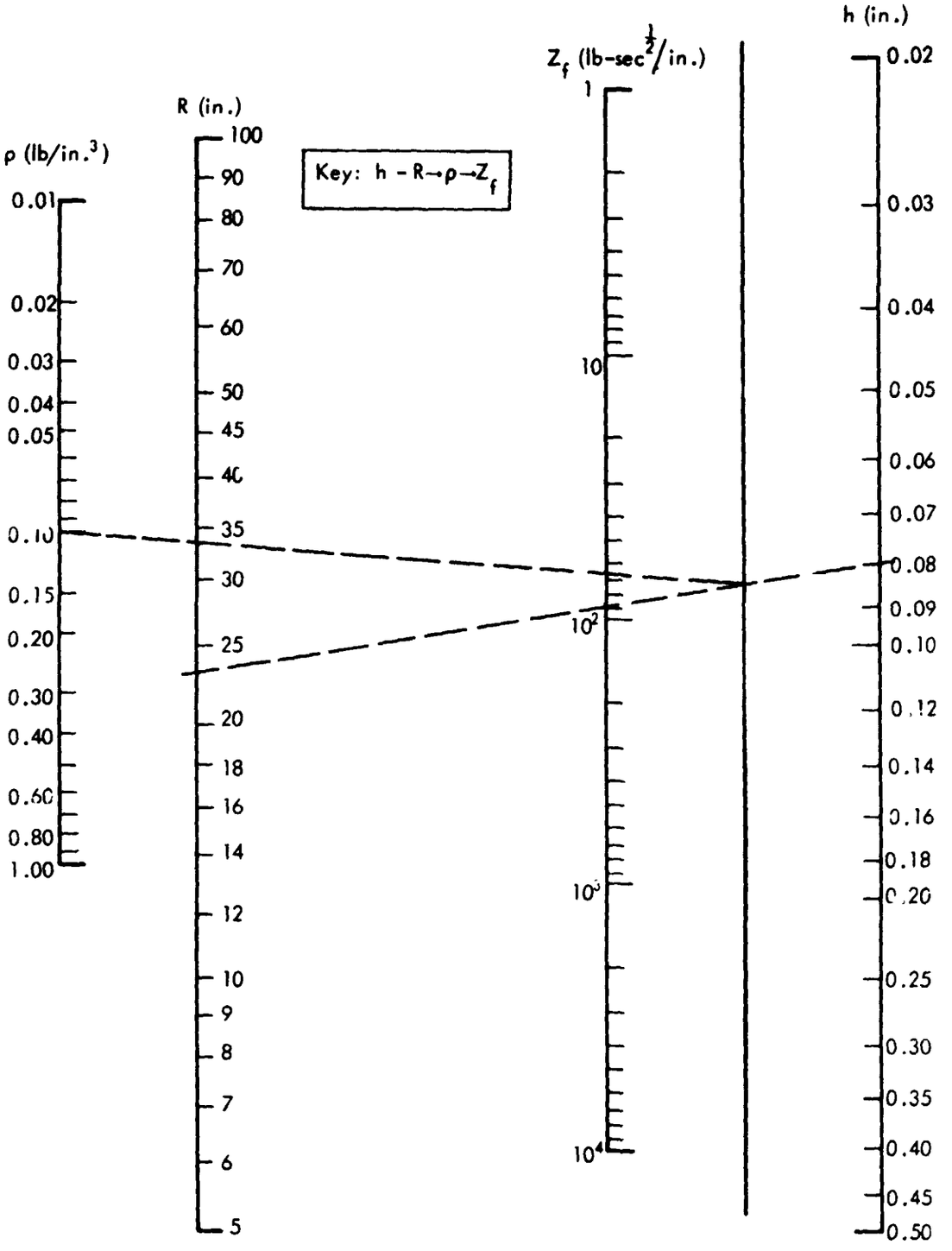

$$Z_f = \frac{4}{\sqrt{3}} \rho h^2 \sqrt{\frac{E}{\rho}} \left(\frac{E}{\rho R^2}\right)^{\frac{1}{4}} \quad , \quad (E = 10^7 \text{ psi for Al})$$

Figure 4.5. Nomograph for Determining Z_f of Unstiffened Cylinders

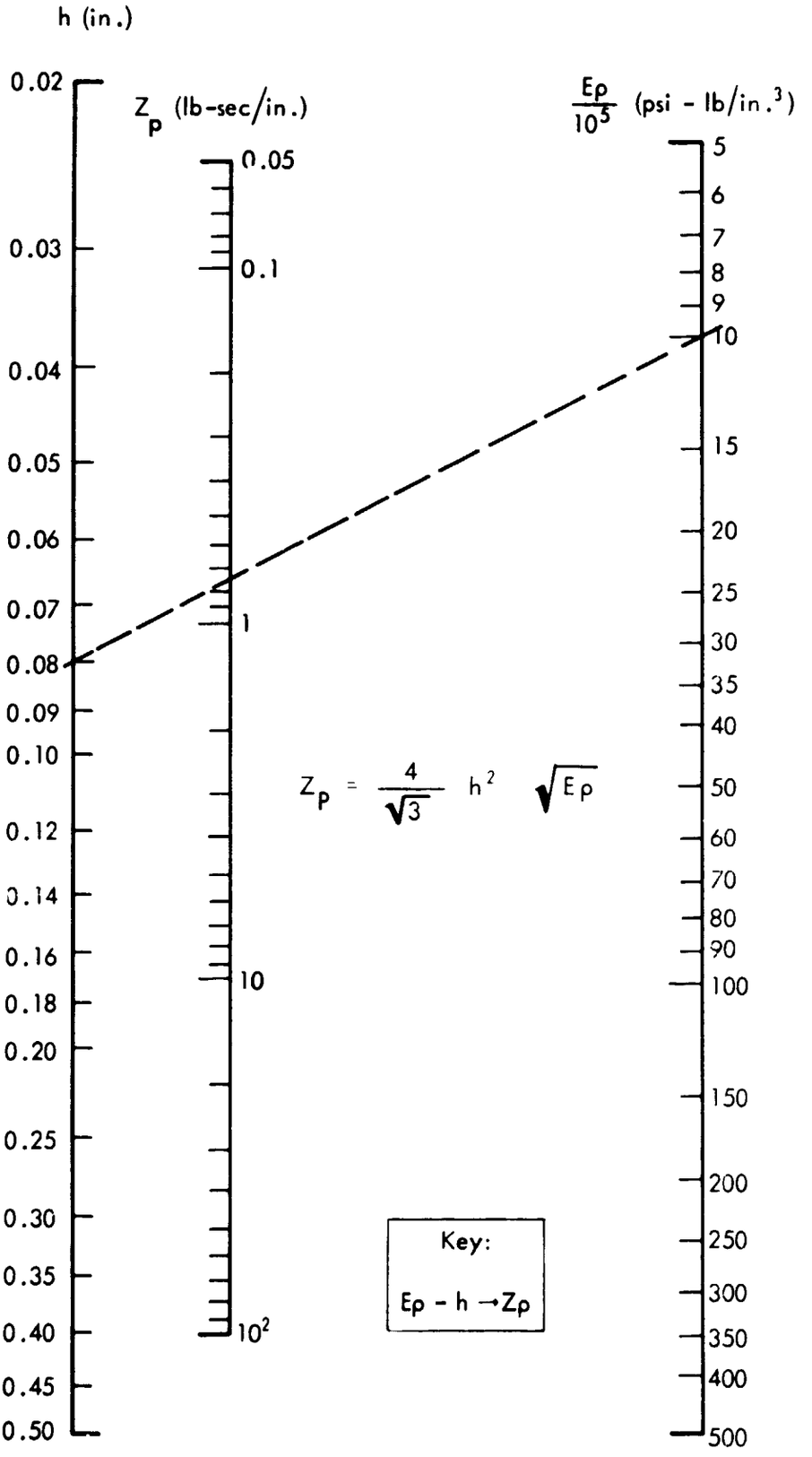

Figure 4.6. Nomograph for Evaluating Impedance of Infinite Plate

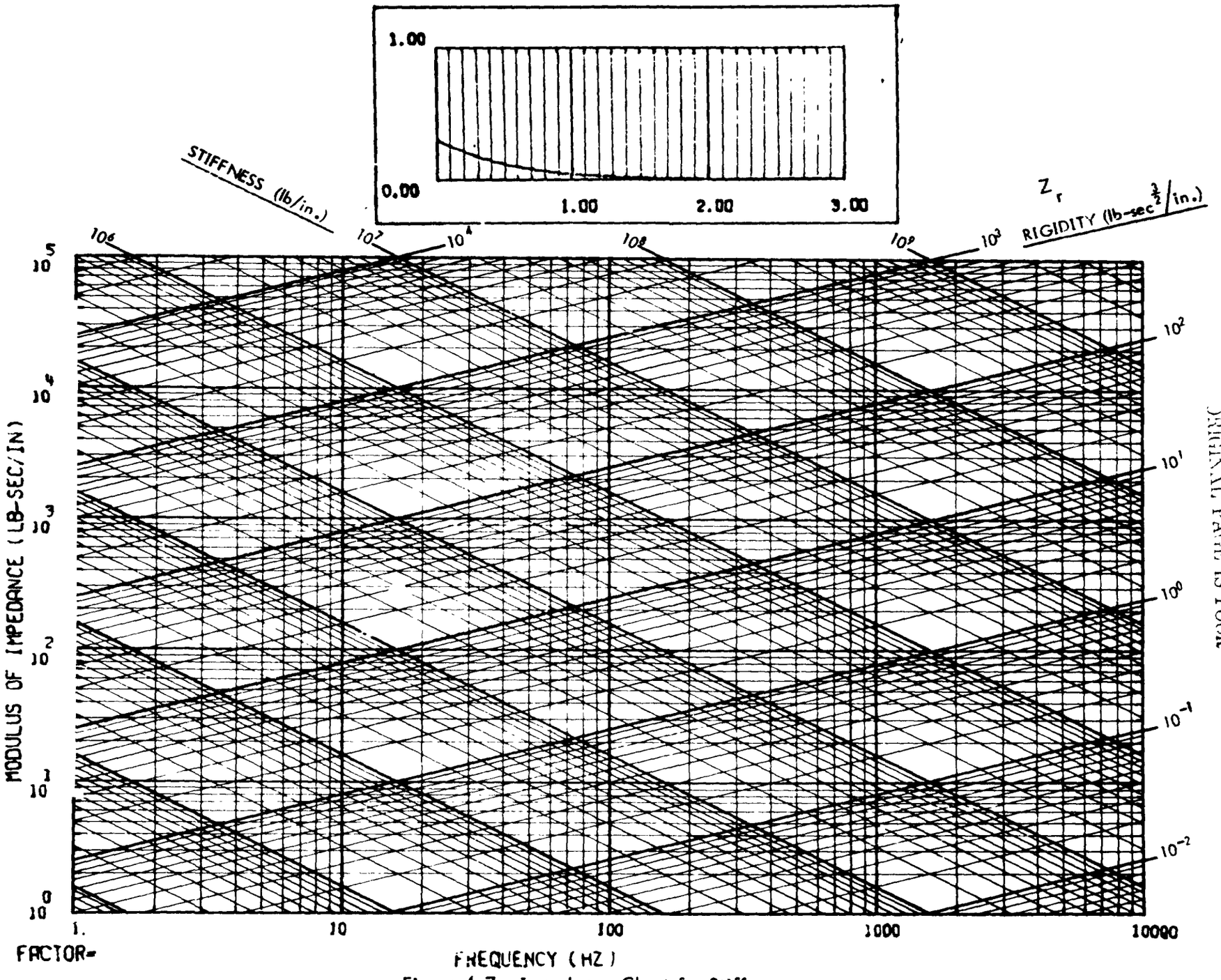

Figure 4.7. Impedance Chart for Stiffeners

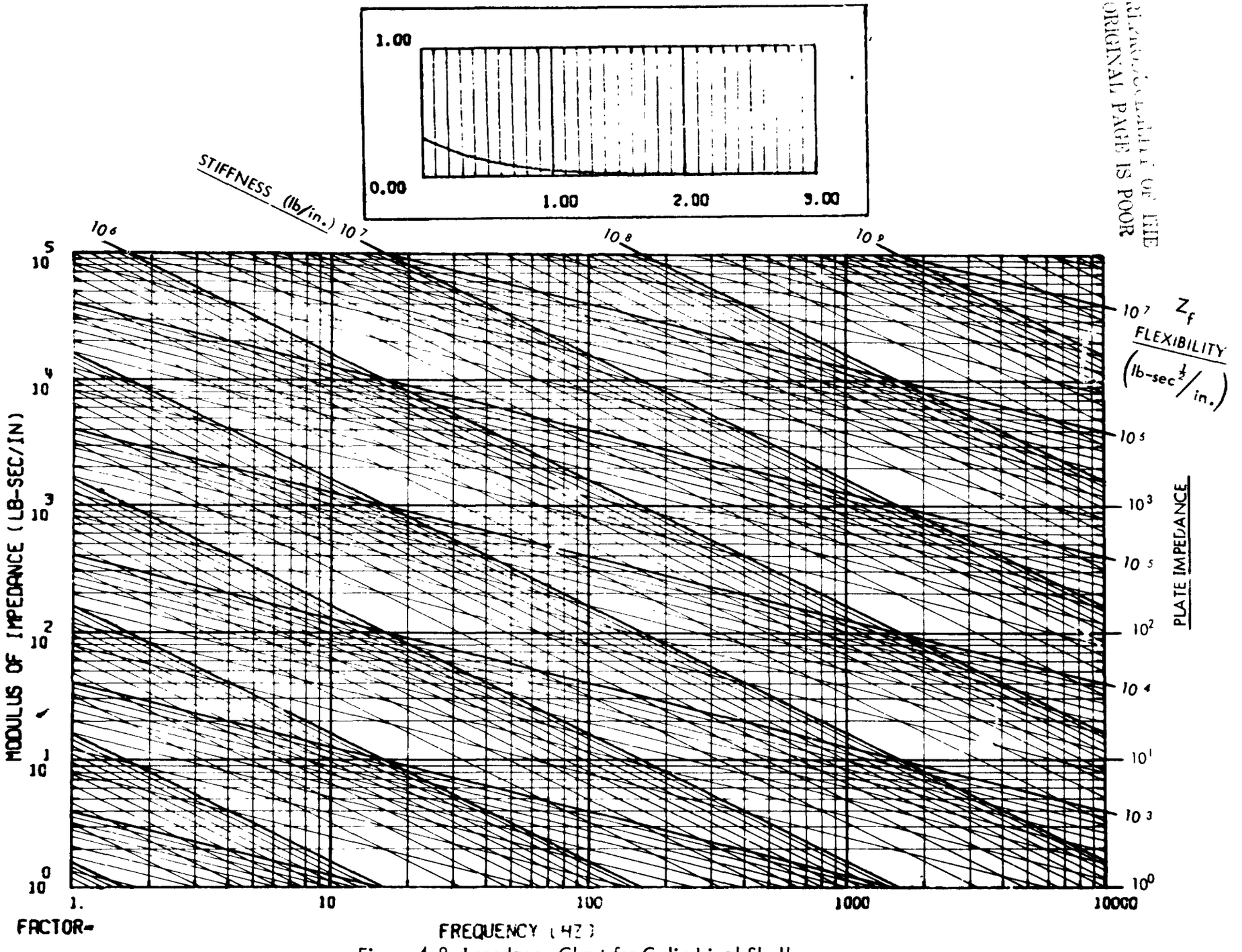

Figure 4.8 Impedance Chart for Cylindrical Shell

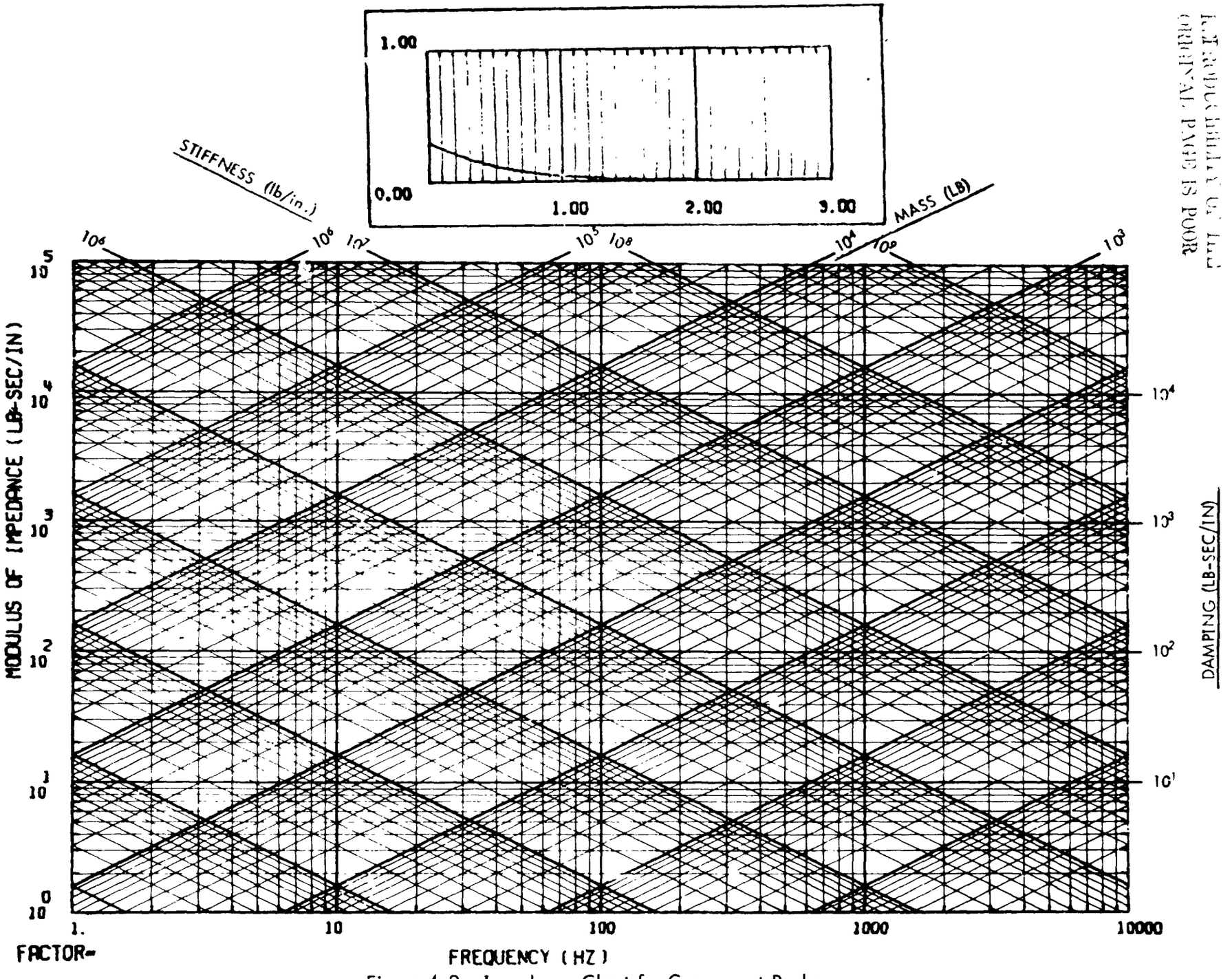

Figure 4.9. Impedance Chart for Component Package

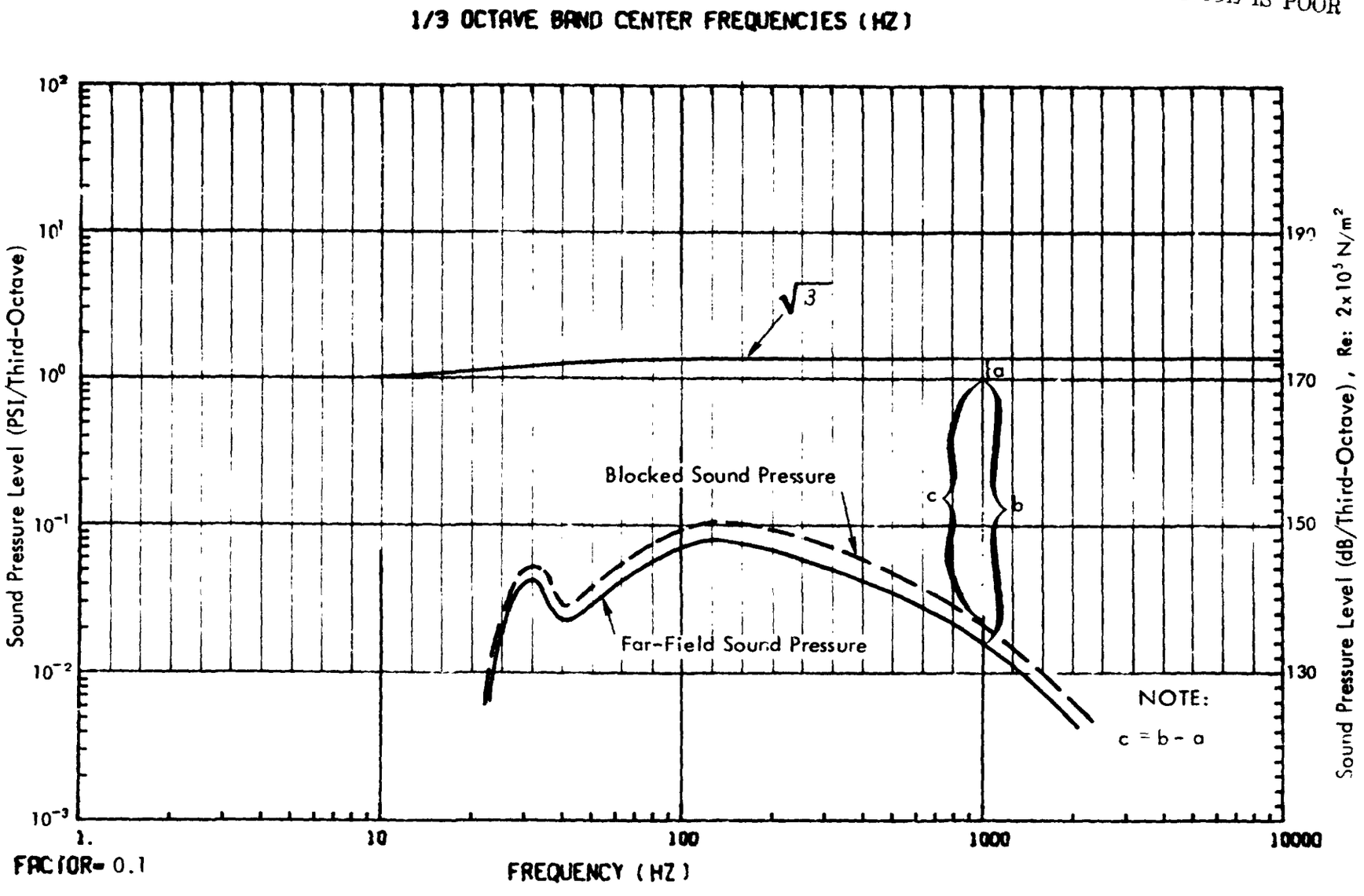

Figure 4.10. Chart for Blocked Pressure Spectrum Computation

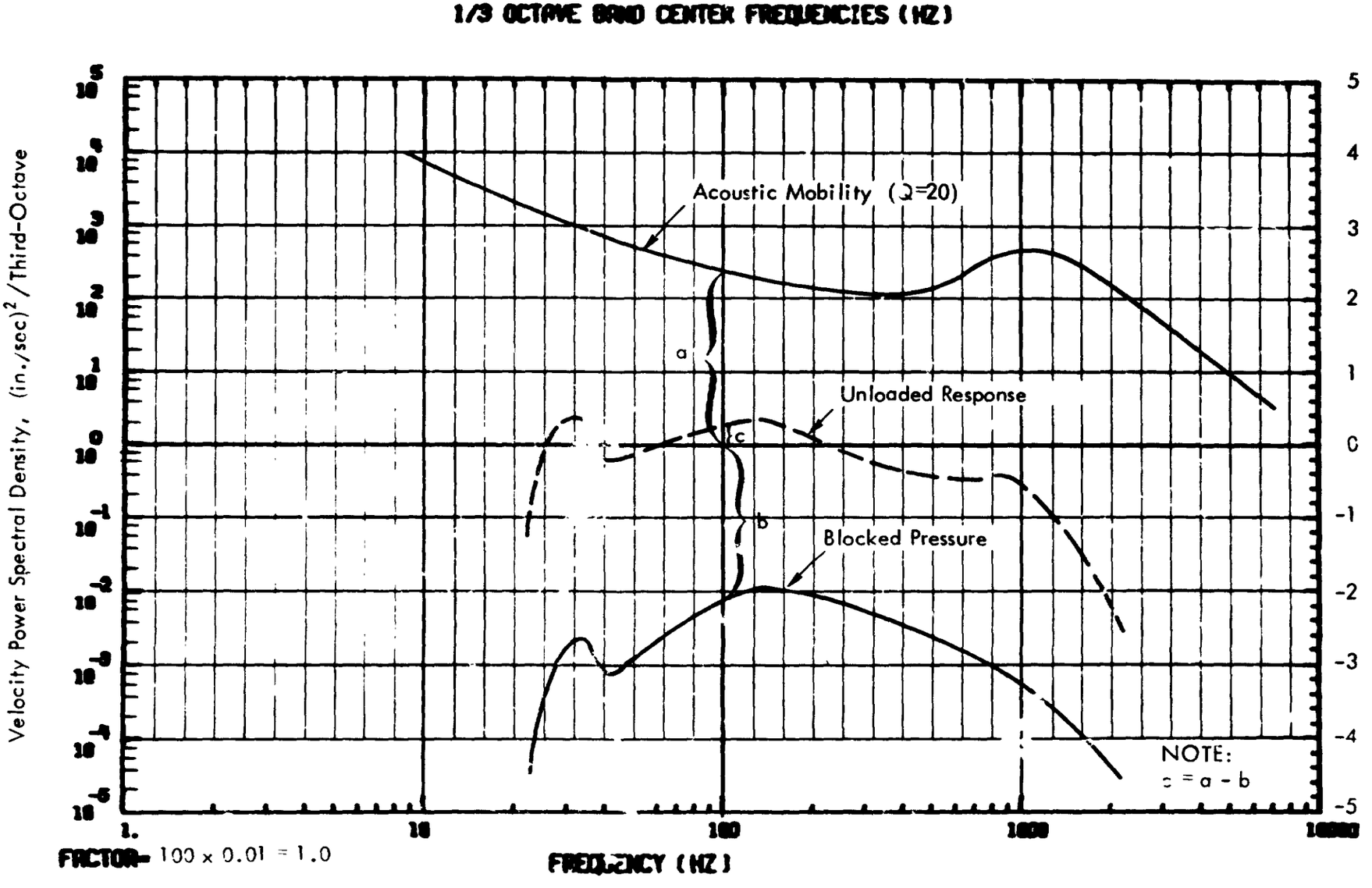

Figure 4.11. Chart for Response Spectrum Computation

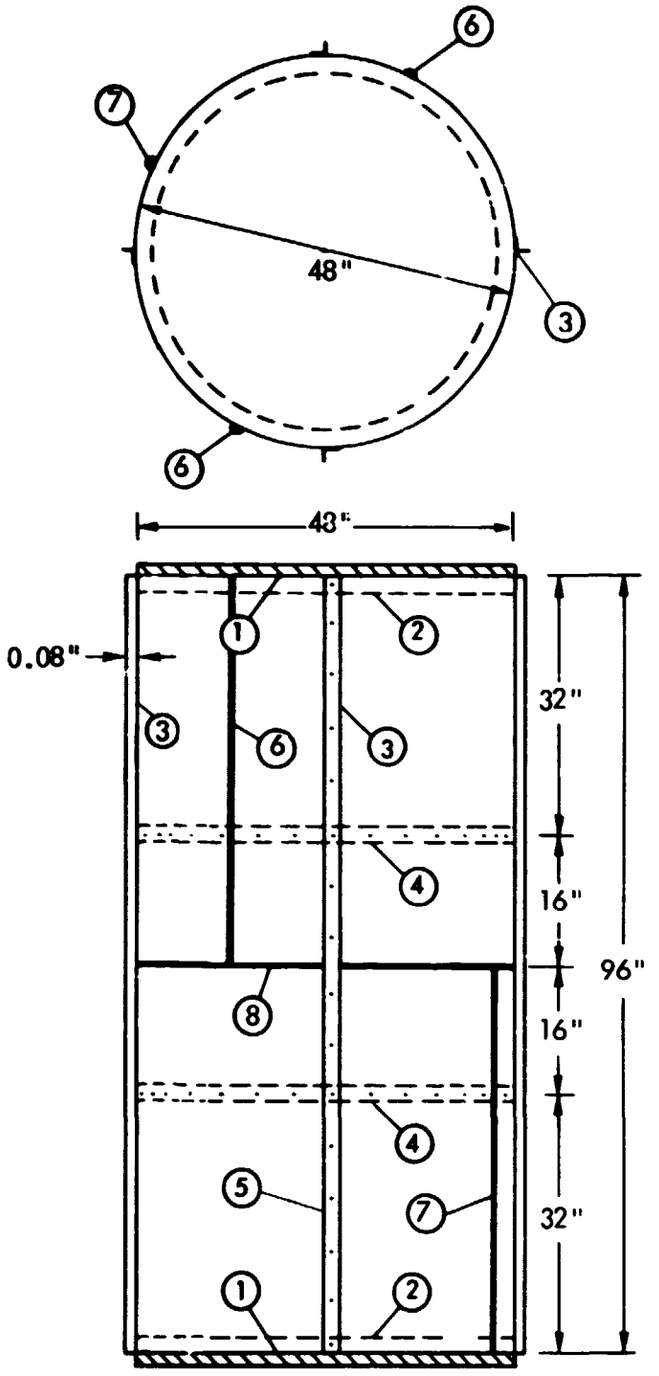

1. Two flat circular plywood bulkheads
2. Two angle section end rings
3. Four angle section stringers
4. Two channel section ring frames
5. Pop rivets
6. Upper axial weld lines
7. Lower axial weld lines
8. Circumferential weld line

Figure 5.1. Geometry and Dimensions of Cylindrical Structure

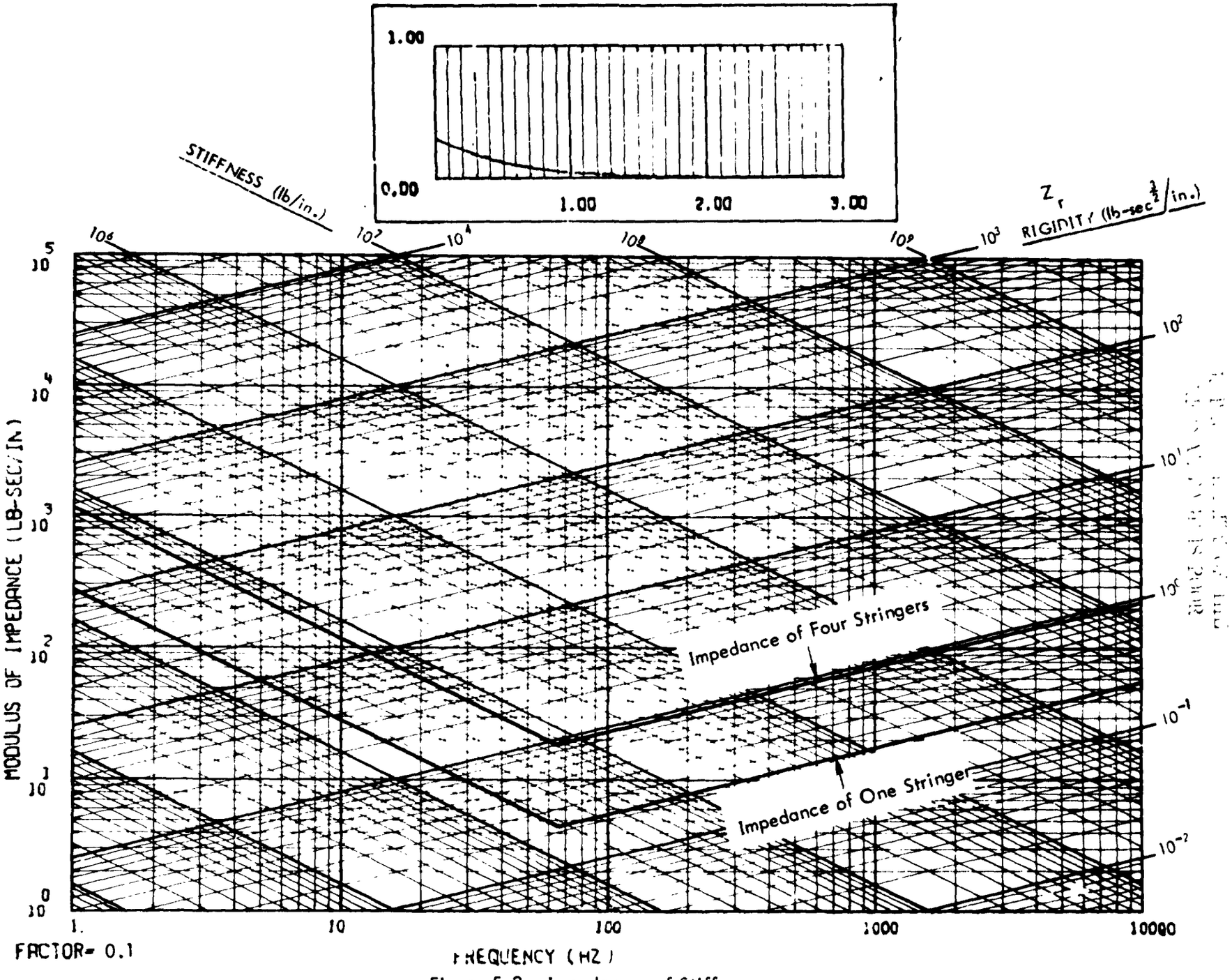

Figure 5.2. Impedances of Stiffeners

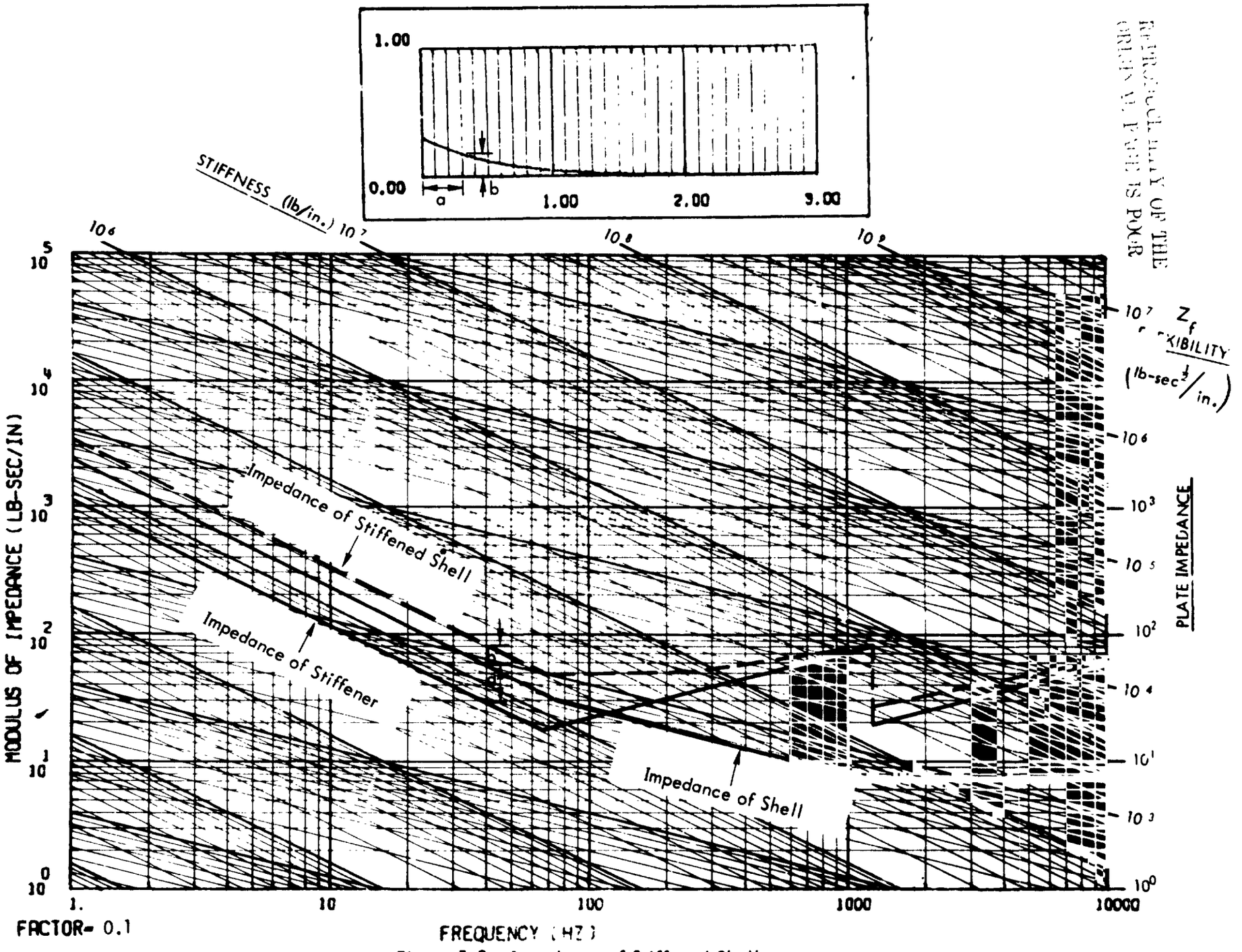

Figure 5.3. Impedance of Stiffened Shells

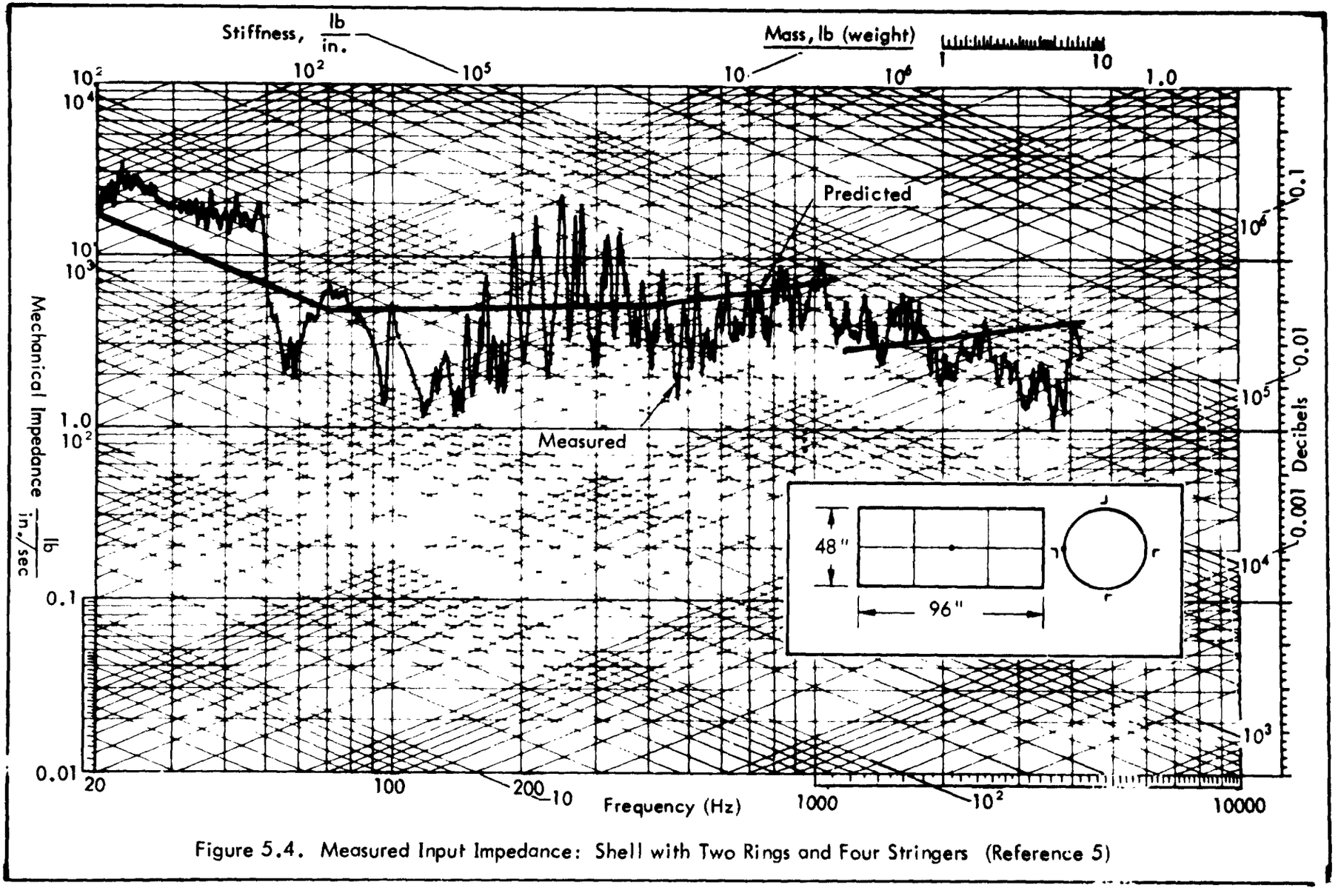

Figure 5.4. Measured Input Impedance: Shell with Two Rings and Four Stringers (Reference 5)

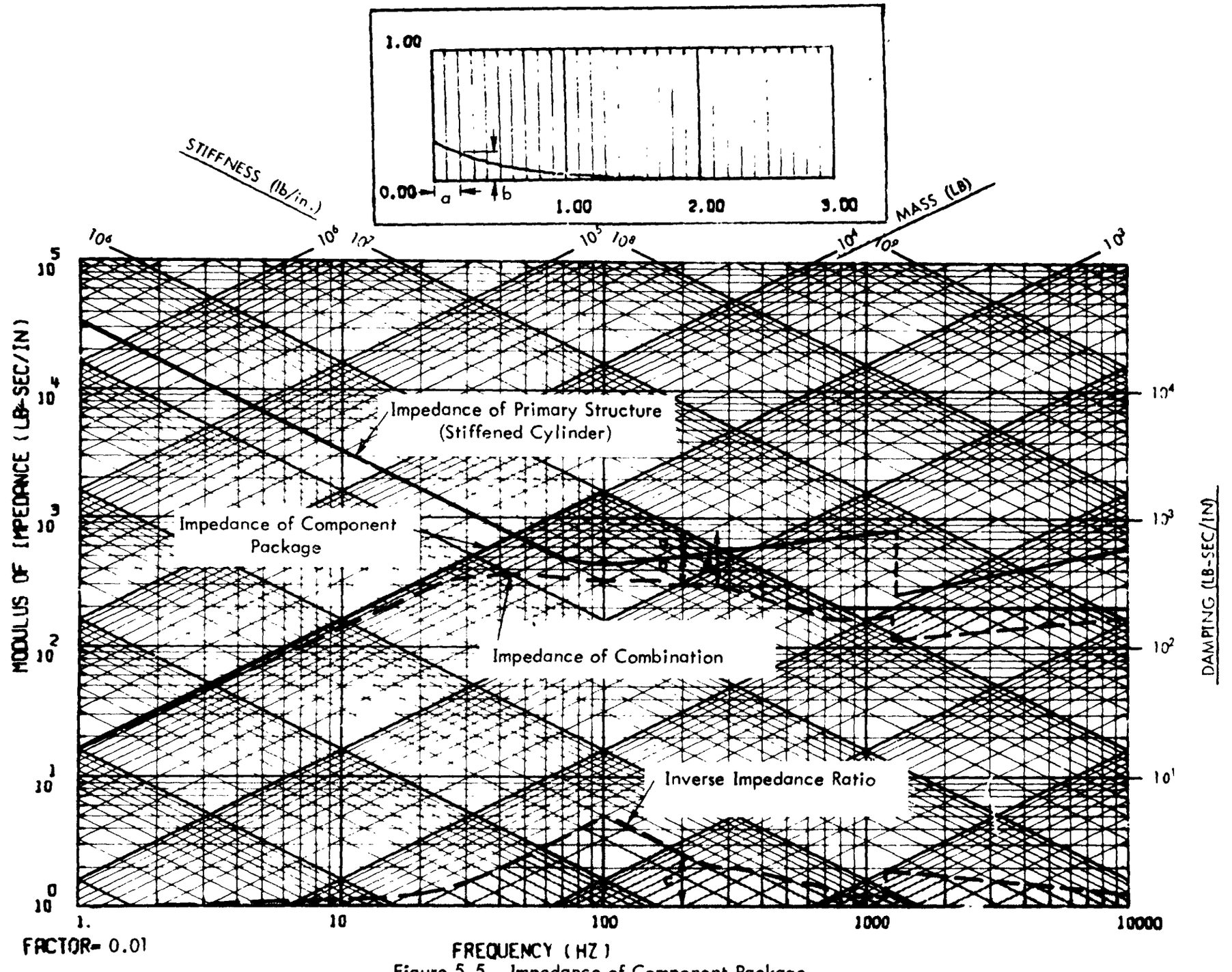

Figure 5.5. Impedance of Component Package

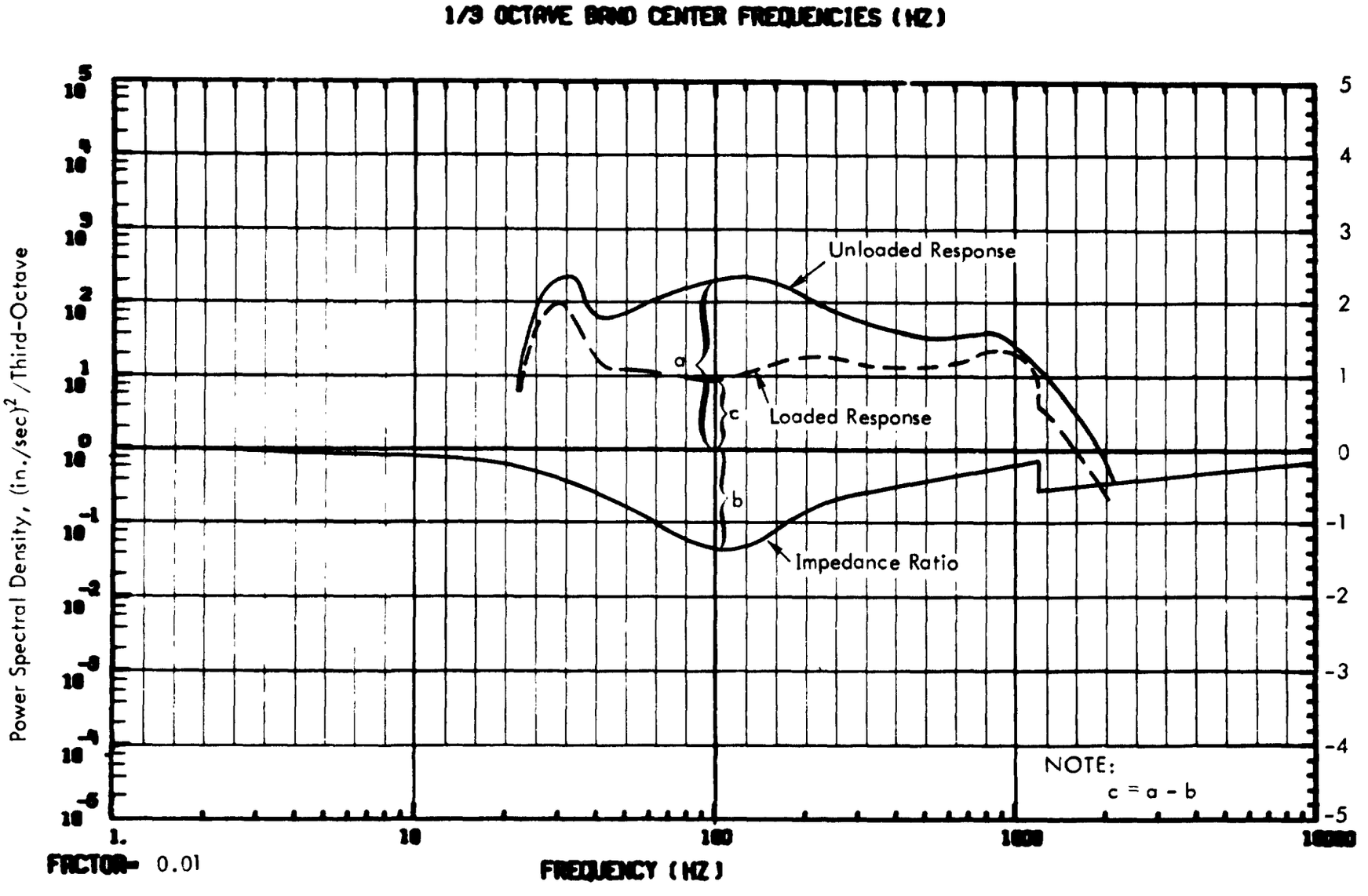

Figure 5.6. Prediction of Loaded Response Spectrum

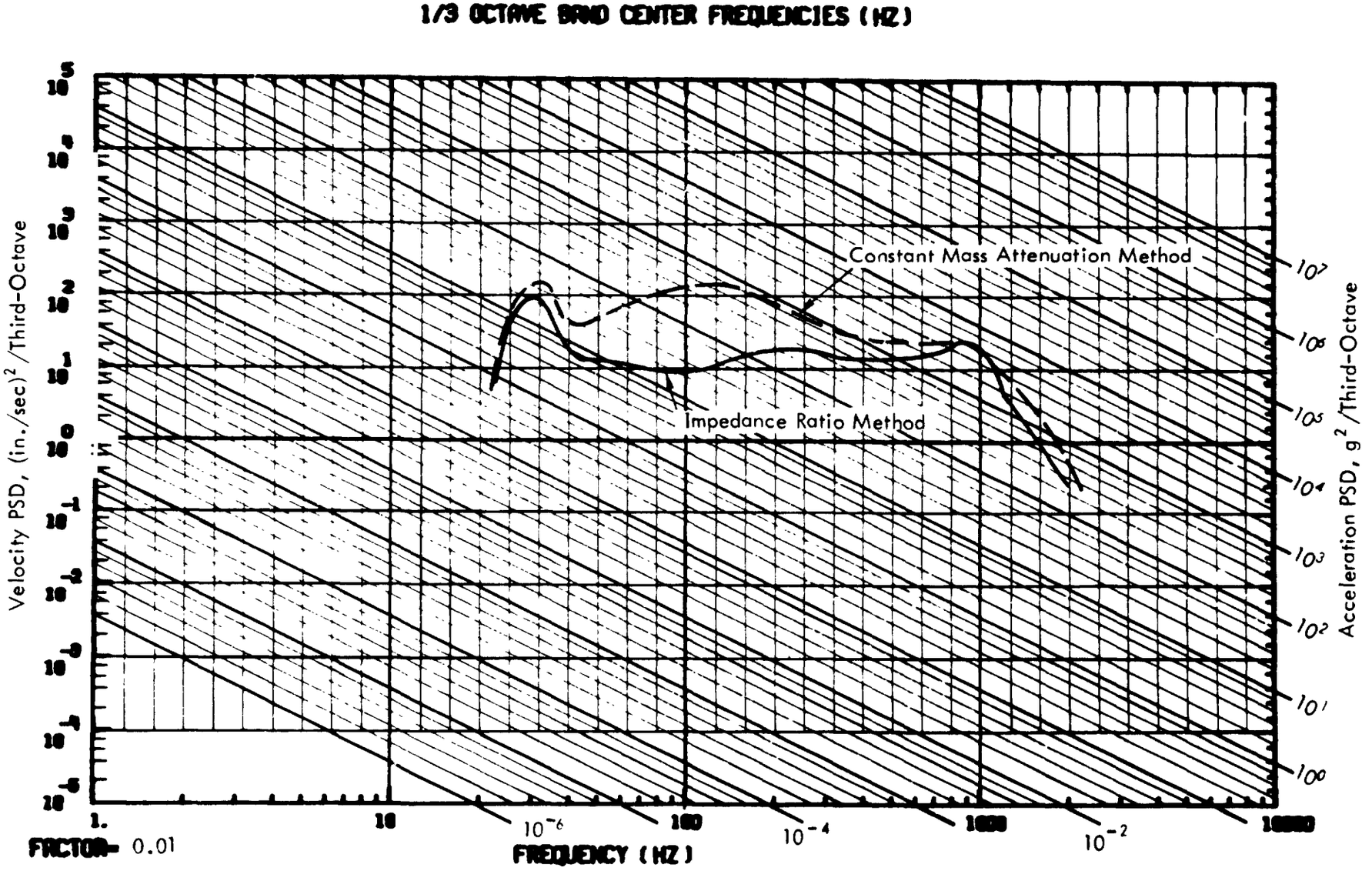

Figure 5.7. Comparison of Loaded Response Spectrum

APPENDIX A

DERIVATION OF IMPEDANCE PREDICTION EQUATION

APPENDIX A

DERIVATION OF IMPEDANCE PREDICTION EQUATION

1.0 INTRODUCTION

The one-dimensional force-spectrum equation is derived based on Thevenin and Norton's theorems (Reference 1). The equation relates the driving force spectrum to external excitation forces, component impedances and dynamic properties of support structures (input impedances and acoustic mobilities). In the subsequent sections, equations which govern the force spectrum of a one-dimensional structural system are presented. The relationship between this system and its analogous vibro-acoustic systems are then established and measurement approaches to acquire needed data are described.

1.1 One-Dimensional Impedance Model of a Structural System

It is assumed that dynamic responses of a structural system subjected to excitations by external forces are predominantly one-dimensional; thus the dynamic characteristics of the structure could be represented by a one-dimensional impedance model as shown in Figure A-1, in which the basic unloaded structure is replaced by an equivalent structural "black box"; external loads are applied at Terminals 1 and 2, and component packages which are treated as load impedances, $Z_L(\omega)$, are attached to Terminals 3 and 4. The corresponding velocities and interaction forces at the attachment points are indicated by $V_L(\omega)$ and $F_L(\omega)$, respectively. The structural impedance model, as shown in Figure A-1, can be represented by the equivalent constant-force model (Thevenin's model) and the constant velocity model (Norton's model) as shown in Figures A-2 and A-3, respectively. The dynamic characteristics at the attachment points (Terminals 3 and 4) are represented by $Z_s(\omega)$, which is defined as support-structure impedance or source impedance. That is, the impedance looking back to the left of Terminals 3 and 4 without any loads attached.

Based on Figure A-2, the force, $F_L(\omega)$, which drives the component $Z_L(\omega)$, can be expressed by the following equation:

$$F_L(\omega) = \frac{Z_L(\omega)}{Z_L(\omega) + Z_s(\omega)} \quad F_0(\omega) \qquad (1)$$

Where $F_0(\omega)$ is the equivalent driving force (blocked force) developed at Terminals 1 and 2 if the load impedance at the attachment points (Terminals 3 and 4) were infinite, i.e., if Terminals 3 and 4 were fixed to a rigid foundation. The corresponding velocity $V_L(\omega)$ of the attached load is:

$$V_L(\omega) = \frac{F_0(\omega)}{Z_L(\omega) + Z_s(\omega)} \tag{2}$$

But the blocked force $F_0(\omega)$ is not a readily measurable quantity, therefore, it is necessary to find an equivalent term which is suitable for measurement.

By definition, the constant source velocity, $V_0(\omega)$, is the velocity at the attachment terminal with no loads attached. Thus, by setting $Z_L(\omega)$ in Equation (2) to zero, the source velocity is determined by the following equation:

$$V_0(\omega) = \frac{F_0(\omega)}{Z_s(\omega)} \tag{3}$$

or

$$F_0(\omega) = V_0(\omega) \cdot Z_s(\omega) \tag{4}$$

Substituting Equation (4) into Equation (2), and the resulting equation for load velocity $V_L(\omega)$ becomes:

$$V_L(\omega) = V_0(\omega) \cdot \left[\frac{1}{1 + Z_L(\omega)/Z_s(\omega)} \right] \tag{5}$$

Equation (5) shows that the load velocity spectrum is equal to the velocity spectrum of the unloaded structure multiplied by the impedance ratio of the support structure to the component package. The term $1/[\,1 + Z_L(\omega)/Z_s(\omega)\,]$ serves as a magnification factor and its value will approach unity when the source impedance $Z_s(\omega)$ becomes infinite. All of the above quantities can be obtained through measurement techniques.

1.2 Structural Responses to Acoustic Excitations

Responses of structures to acoustic excitations, as shown in Figure A-4, can be expressed by the following equations (Reference 2):

$$\phi_{\dot{x}}(\vec{r},\omega) = \sum_m \sum_m \frac{\phi_m(\vec{r})\,\phi_n(\vec{r}) \cdot A^2}{Z_m(\omega)\,Z_n(\omega)^*}\,\phi_{p_0}(\omega)\,J_{mn}^2(\omega) \qquad (6)$$

where

$\phi_{\dot{x}}(\vec{r},\omega)$ = Velocity power spectral density at point r

$\phi_{p_0}(\omega)$ = Power spectral density of reference sound pressure which is assumed to be constant over the surface of component mounting locations

A = Surface area

$Z_m(\omega)$ = Modal impedance

$$= \frac{K_m}{i\omega}\left[1 - \left(\frac{\omega}{\omega_m}\right)^2 + \frac{i}{Q_m}\left(\frac{\omega}{\omega_m}\right)\right]$$

$Z_n(\omega)^*$ = Complex conjugate of $Z_n(\omega)$

$J_{mn}^2(\omega)$ = Joint acceptance function of the mn^{th} mode

$$= \iint_{s\ s'} \frac{\phi_m(\vec{s})\,\phi_n(\vec{s'})}{A^2}\,\frac{\phi_p(\vec{s},\vec{s'},\omega)}{\phi_{p_0}(\omega)}\,d\vec{s}\,d\vec{s'}$$

$d\vec{s},\ d\vec{s'}$ = Infinitesimal area vectors

$\phi_p(\vec{s},\vec{s'},\omega)$ = Cross-power spectral density of the sound pressure field

$\phi_m(\vec{r}),\ \phi_m(\vec{s})$ = Normal mode at $\vec{r}$ and $\vec{s}$, respectively

K_m = Generalized stiffness

ω_m = m^{th} natural frequency = $\sqrt{K_m / M_m}$

M_m = Generalized mass = $\int_s \rho(\vec{s})\,\phi_m^2(\vec{s})\,d\vec{s}$

Q_m = Generalized dynamic magnification factor

ρ = Surface mass density

By rearranging terms in Equation (6), the acoustic velocity mobility is obtained:

$$\left| \alpha_{\dot{x}} (\vec{r}, \omega) \right|^2 = \frac{\Phi_{\dot{x}}(\vec{r}, \omega)}{\Phi_{p_0}(\omega)} = \sum_m \sum_n \frac{\phi_m(\vec{r}) \phi_n(\vec{r}) \cdot A^2}{Z_m(\omega) Z_n(\omega)} J_{mn}^2(\omega) \tag{7}$$

In practice, velocity responses of a complex structure subjected to acoustic excitations may be expressed as follows:

$$\Phi_{\dot{x}}(\vec{r}, \omega) = \Phi_p(\vec{r}, \omega) \left| \alpha_{\dot{x}}(\vec{r}, \omega) \right|^2 \tag{8}$$

where $\Phi_p(\vec{r}, \omega)$ is the blocked sound pressure spectrum at $\vec{r}$.

To determine the acoustically induced response spectra $\Phi_L(\vec{r}, \omega)$ at attachment points, it is necessary to transform a vibro-acoustic system to an equivalent one-dimensional impedance model, so that Equation (5) can be applied directly to determine $\Phi_L(\vec{r}, \omega)$. Such a transformation is illustrated in Figure A-5 . The equivalent one-dimensional model is represented by a support structural impedance, $Z_s(\vec{r}, \omega)$, the component impedance, $Z_L(\vec{r}, \omega)$, and an equivalent blocked force spectrum, $\Phi_L(\vec{r}, \omega)$. Applying Equations (4), (5) and (8) to the above system, the blocked force spectra equation is obtained:

$$\text{Blocked Force Spectra: } \Phi_L(\vec{r}, \omega) = \Phi_{\dot{x}}(\vec{r}, \omega) \cdot \left| Z_s(\vec{r}, \omega) \right|^2 \tag{9}$$

and the load velocity response spectra is presented as follows:

$$\Phi_{\dot{x}}(\vec{r}, \omega) = \Phi_p(\vec{r}, \omega) \cdot \left| \alpha_{\dot{x}}(\vec{r}, \omega) \right|^2 \cdot \left| \frac{1}{1 + Z_L(\vec{r}, \omega) / Z_s(\vec{r}, \omega)} \right| \tag{10}$$

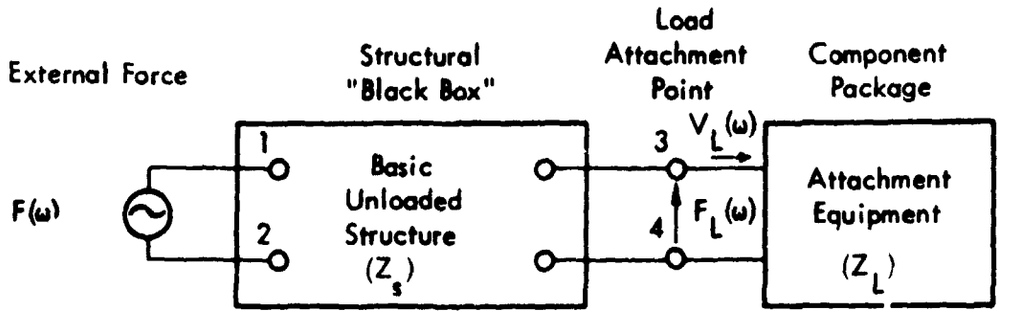

Figure A-1. One-Dimensional Impedance Model of a Structural System

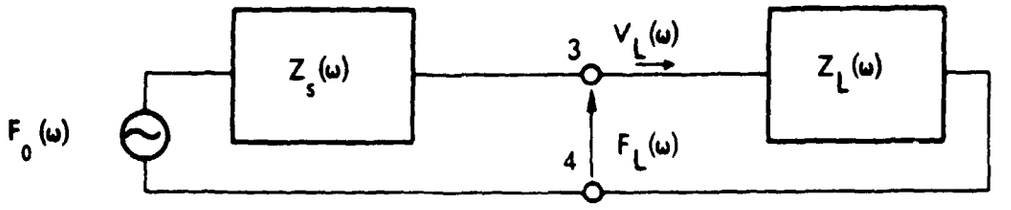

Figure A-2. Equivalent-Constant Force Model

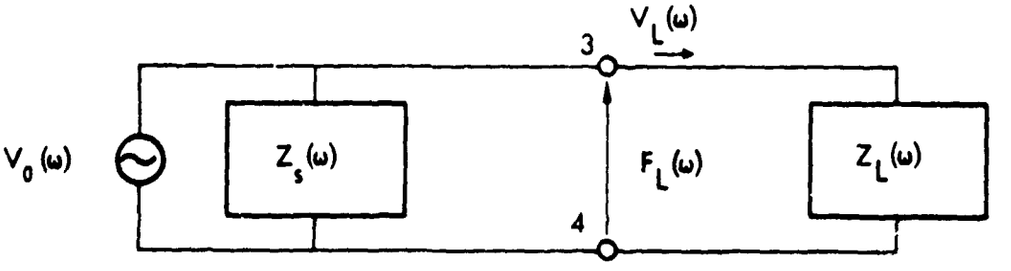

Figure A-3. Equivalent-Constant Velocity Model

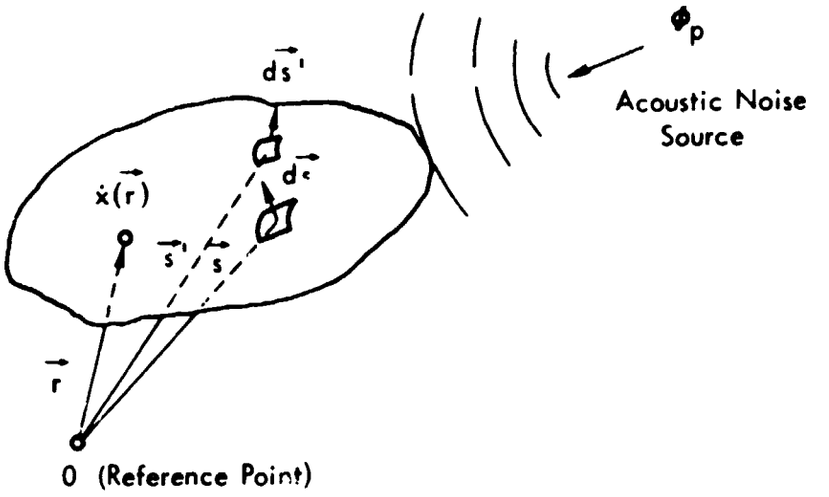

Figure A-4. Structure Response Subject to Acoustic Excitation

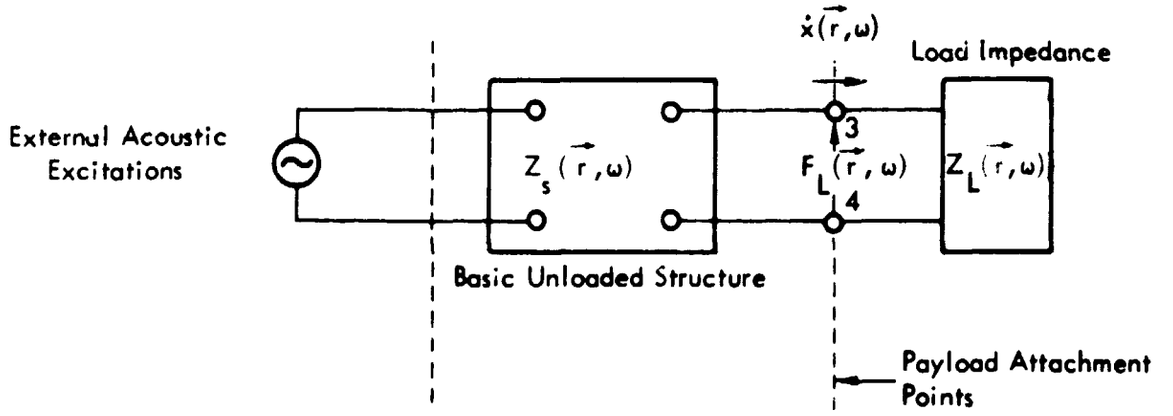

(a) A Typical Structure Subject to the Acoustic Excitations

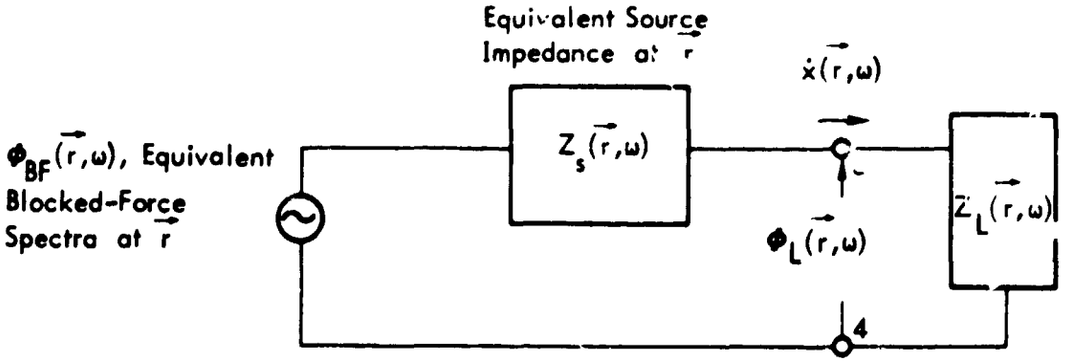

(b) An Equivalent One-Dimensional Impedance Model

Figure A-5. One-Dimensional Model of a Structural System Subject to Acoustic Excitations

REFERENCES

1. Tang, K.Y., Alternating-Current Circuits, International Textbook Company, Scranton, Pennsylvania, 1955.

2. Powell, A., "On the Response of Structures to Random Pressures and to Jet Noise in Particular," Random Vibration, Vol. I, Chapter 8, John Wiley and Sons, Inc., New York, 1958.

APPENDIX B

IMPEDANCE OF PAYLOAD STRUCTURE

APPENDIX B

IMPEDANCE OF PAYLOAD STRUCTURE

The Payload structure can be assumed as a lumped-mass system. The mathematical model is shown in Figure B-1 and the differential equations of motion can then be written as:

$$\begin{cases} M\ddot{x} + C(\dot{x} - \dot{y}) + K(x - y) = 0 \\ \\ C(\dot{x} - \dot{y}) + K(x - y) = -Fe^{i\omega t} \end{cases} \tag{1}$$

in which M represents the total mass, K is the stiffness, and C denotes the damping of the system. The frequency of the steady-state motion is the same as the force excitation frequency, ω, therefore, the mechanical impedance of the system is obtained as follows:

$$\begin{aligned} Z = \frac{Fe^{i\omega t}}{\dot{y}} &= \frac{1}{\frac{1}{i\omega M} + \frac{1}{C + \frac{K}{i\omega}}} \\ &= i\omega M \frac{\left[1 + \frac{i}{Q}\left(\frac{\omega}{\omega_0}\right)\right]}{\left[\left(1 - \frac{\omega^2}{\omega_0^2}\right) + \frac{i}{Q}\left(\frac{\omega}{\omega_0}\right)\right]} \\ &= \frac{K}{i\omega} \frac{\left[1 + \frac{i}{Q}\left(\frac{\omega}{\omega_0}\right)\right]}{\left[\left(1 - \frac{\omega_0^2}{\omega^2}\right) - \frac{i}{Q}\left(\frac{\omega_0}{\omega}\right)\right]} \end{aligned} \tag{2}$$

where

$\omega_0 = \sqrt{K/M}$ = resonance frequency of undamped system

$Q = \sqrt{KM}/C$ = dynamic magnificant factor

For the region, $\omega \ll \omega_0$, Equation (2) can be approximated by:

$$Z \simeq i\omega M \tag{3}$$

Equation (3) shows that the impedance is a purely mass line. For the region, $\omega \gg \omega_0$, it is possible to obtain an approximate formula for the impedance and this approximation yields the following impedance formula:

$$Z \simeq \frac{K}{i\omega}\left[1 + \frac{i}{Q}\left(\frac{\omega}{\omega_0}\right)\right] = C + \frac{K}{i\omega} \tag{4}$$

At high frequencies, the impedance became asymptotic to a constant value and 's equal to the damping value.

$$Z \simeq C \tag{5}$$

A typical example of the component impedance plot is shown in Figure B-2 as a function of the frequency of the driving force. The approximated curve is also shown in the same figure for comparison.

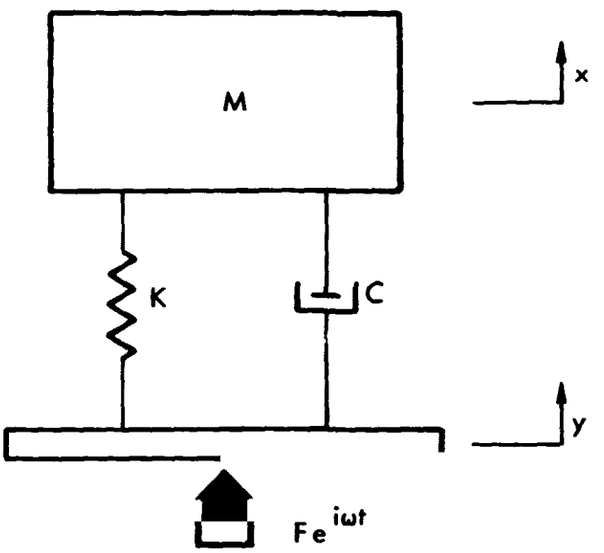

Figure B-1. Mass-Spring – Dashpot Model

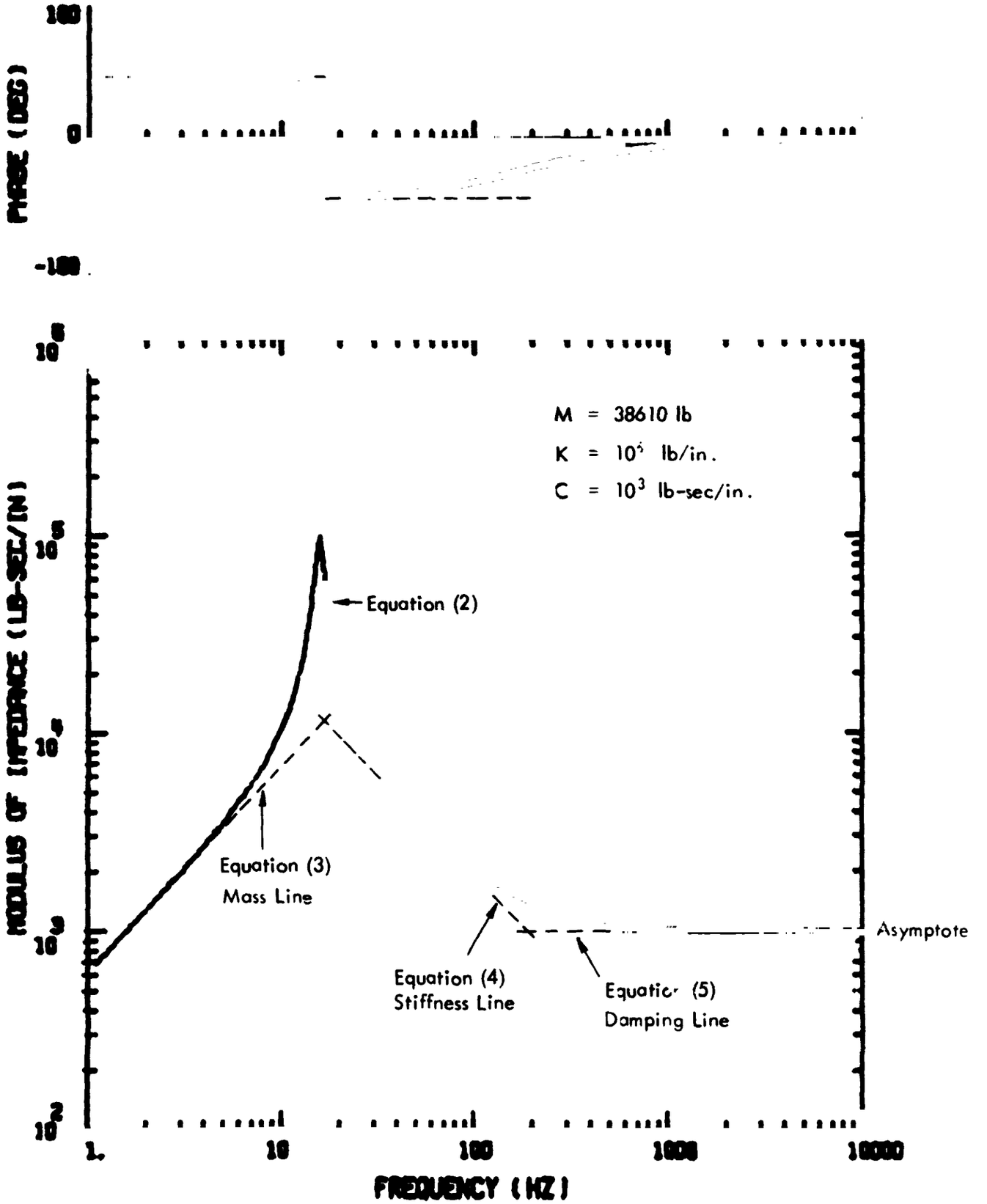

Figure B-2. Impedance of Component Package

APPENDIX C

APPROXIMATE EQUATIONS RELATED TO DYNAMIC CHARACTERISTICS OF STRUCTURES

APPENDIX C

APPROXIMATE EQUATIONS RELATED TO DYNAMIC CHARACTERISTICS OF STRUCTURES

Brief discussions of approximate equations on input impedances, resonant frequencies and modal densities are given in this appendix. The structural elements considered in the derivation consist of the following categories:

- Beams (or stringers),
- Circular ring frames, and
- Unstiffened cylindrical shells.

The derivation of the approximate equations is based on the assumption that the thickness of cylindrical shells is small such that the thin shell theories are valid and the direction of vibratory response under consideration is referred to as that normal to the skin. The evaluation of the input impedances may be subdivided into three different frequency ranges as below:

- Low frequency range or frequencies below the fundamental frequency of the shell,
- Intermediate frequency range, and
- High frequency range or frequencies above the ring frequency of the shell.

Beam (or Stringer) Impedances — The static stiffness of a beam defines the input impedance at frequencies below the fundamental resonant frequency of the beam. The static stiffness at the mid-length point of a simply supported beam is given by:

$$K = 48 \frac{EI}{\ell^3} \tag{1}$$

where

E = Young's modulus of elasticity

I = moment of inertia of stringer cross-section

ℓ = effective length of stringer*

---

* Note: If the distance ℓ, between two adjacent supports is different from the entire length of a stringer, the stiffness should be computed in according to the shortest support distance.

Then the input impedance is obtained as:

$$Z = K/i\omega \tag{2}$$

where

ω = circular frequency

$i = \sqrt{-1}$

The fundamental resonance frequency of the beam can be computed from the following equation:

$$f_L = \frac{1}{2\pi}\left(\frac{\pi}{\ell}\right)^2 \sqrt{\frac{EI}{\rho A}} \tag{3}$$

where

ρ = mass density

A = cross-section area of stringer

At high frequencies or frequencies above the fundamental frequency, the average input impedance can be approximated as the characteristic impedance of an infinite beam and is given by Cremer (Reference 1) as follows:

$$Z = 2(1+i)\,\rho A \left(\frac{EI}{\rho A}\right)^{1/4} \sqrt{\omega} \tag{4}$$

The impedance curve defined by the above equation is represented by the line that passes through the points of inflection of the impedance curve as shown in Figure C-1. The peaks and valleys are proportional to the damping coefficient, Q, and are located above or below the average impedance line; their amplitudes, in respect to the average impedance line, decrease with increasing frequency and the order of reduction in relative amplitudes is proportional to $1/\sqrt{\omega}$. The equation used to compute the ratio of peak values is defined as:

$$\frac{|Z_{peak}|}{|Z_{avg}|} = 4\sqrt{2}\,\frac{1}{\ell}\left(\frac{EI}{\rho A}\right)^{1/4}\frac{Q}{\sqrt{\omega}} \tag{5}$$

Ring Impedances — The in-plane static stiffness of a simply supported ring is given by (Reference 2):

$$K = \frac{EI}{0.15R^3} \tag{6}$$

where

I = moment of inertia of ring cross-section area

R = median radius of ring

However, the low frequency response of a free ring is associated with rigid-body motion which is along the mass line in the impedance plot and is given by:

$$Z = i\omega M \tag{7}$$

where M is the total mass of the ring and is expressed as:

$$M = 2\pi \rho R A$$

A = cross-section area of ring

The lowest resonant frequency of the fundamental mode of rings is defined as follows:

$$f_L = 0.427 \frac{1}{R^2} \sqrt{\frac{EI}{\rho A}} \tag{8}$$

at frequencies above the fundamental frequency, the impedance curve approaches the impedance of an infinite beam whose value is given by:

$$Z = i\, 2\sqrt{2}\ \rho A \left[\frac{EI}{\rho A}\right]^{1/4} \sqrt{\omega} \tag{9}$$

Similarly, the peak responses at resonance frequencies are proportional to structural damping and its peak/average ratio is obtained as:

$$\frac{|Z_{peak}|}{|Z_{avg}|} = 2\sqrt{2}\ \frac{1}{\pi R}\ \left[\frac{EI}{\rho A}\right]^{1/4}\ \frac{Q}{\sqrt{\omega}} \qquad (10)$$

The impedance curve obtained from the approximate equations is illustrated in Figure C-2 along with the analytic solution.

Shell Impedances — The static input stiffness of a simply supported cylindrical shell defines the input impedance at frequencies below the fundamental resonant frequency of the shell. The static point input stiffness at the mid-length of a cylindrical shell can be estimated by the following approximate formula (Reference 3):

$$K = 2.50\ Eh\left(\frac{R}{\ell}\right)^{1/2}\ \left(\frac{h}{R}\right)^{5/4} \qquad (11)$$

where

h = thickness of shells

R = radius of shell

ℓ = effective length of shell

E = Young's modulus of elasticity

The fundamental frequency of a thin shell with simply supported ends is

$$f_L = 0.375\ \frac{C_L}{\ell}\ \left(\frac{h}{R}\right)^{1/2} \qquad (12)$$

where

C_L = speed of sound in shell wall

$$= \sqrt{\frac{E}{\rho\,(1-\nu^2)}}$$

and

ρ = mass density

ν = Poisson's ratio

At high frequencies, the impedance becomes asymptotic to a constant value and is given by the expression:

$$Z_p = \frac{4}{\sqrt{3}} \rho h^2 C_L \tag{13}$$

which is identical to the impedance of a semi-infinite plate of width πR. The frequency for which the corresponding mode shape shows no dependence on the axial direction is defined as the ring breathing frequency. The equation used to compute the ring frequency is given by:

$$f_R = \frac{1}{2\pi} \frac{C_L}{R} \tag{14}$$

Within the intermediate frequency range, which extends from the fundamental frequency to the ring frequency, the impedance curve can be approximated by the straight line which joins two points representing the input impedances at the fundamental frequency and the ring frequency, respectively. The expression which describes this impedance curve was derivated and is expressed below.

$$|Z| \simeq Z_p \cdot \left(f_R/f\right)^{1/2}$$

$$= \frac{4}{\sqrt{3}} \rho h^2 C_L^{3/2} \Big/ \sqrt{R\omega} \tag{15}$$

An alternate theoretical method employing the concept of the modal density can also be used for estimating the impedance at intermediate frequencies. The modal density of a structure is defined as the average number of resonant frequencies that occur within a unit frequency band. The inverse of the modal density is equal to the average separation between resonant frequencies. Heckle (Reference 4) derived a closed form expression for the modal density of a uniform cylindrical shell using a simple approximation to the frequency equation; and these expressions are used to obtain the average separation between resonant frequencies (see also Reference 5) as follows:

$$\Delta f = \frac{8\pi}{9\sqrt{3}} \frac{h}{\ell} \frac{f_R^{3/2}}{f^{1/2}} \quad \text{for} \quad f < f_R \tag{16}$$

and the input impedance can be approximated by the following equation (Reference 6).

$$|Z| = \frac{2}{\pi} \cdot 2\pi\Delta f \cdot M_m$$

$$= \frac{8\pi}{9\sqrt{3}} \rho h^2 C_L^{3/2} \Big/ \sqrt{R\omega} \tag{17}$$

in which M_m represents the modal mass and is approximately equal to one-quarter of the total mass of shell.

Comparison of Equations (15) and (17) shows that the theoretically derived expression in Equation (15) is essentially the same result as the empirical equation obtained by fitting the desired curve. A comparison of the resulting impedances obtained either from the approximate and analytical equations is shown in Figure C-3.

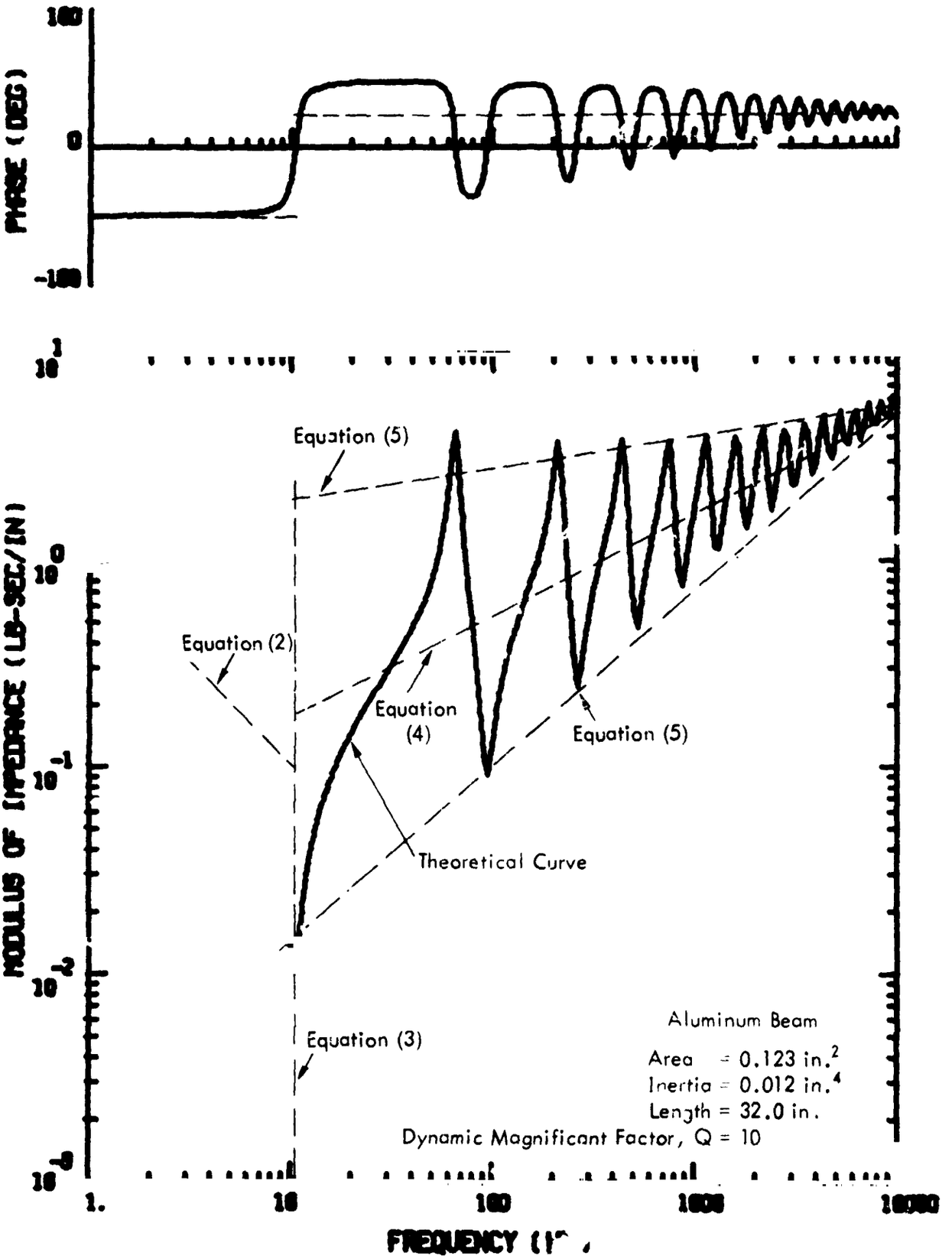

Figure C-1. Comparison of Design Equations with the Analytic Solution for the Impedance of Beam-Type Structures

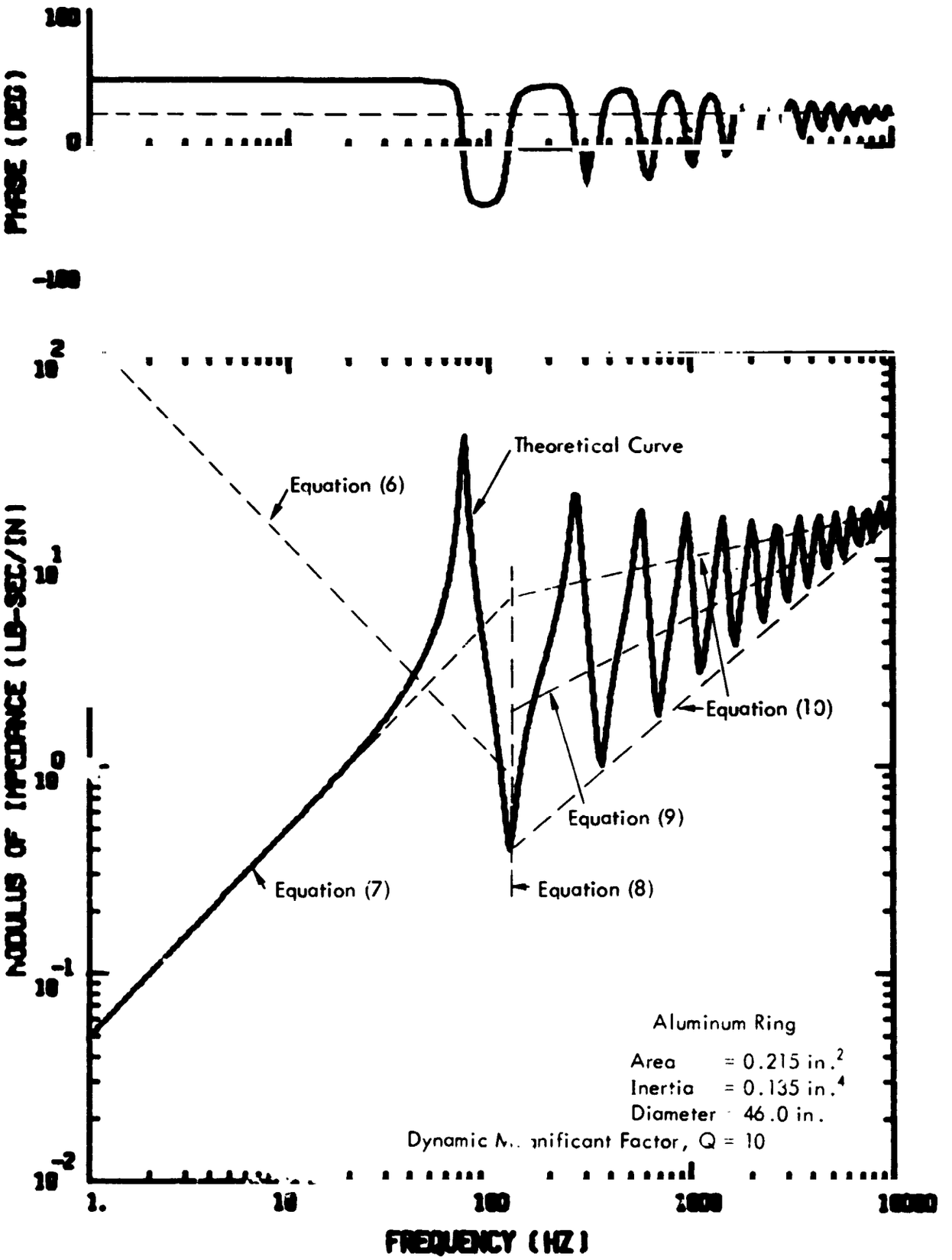

Figure C-2. Comparison of Design Equations with the Analytic Solution for the Impedance of Ring-Type Structures

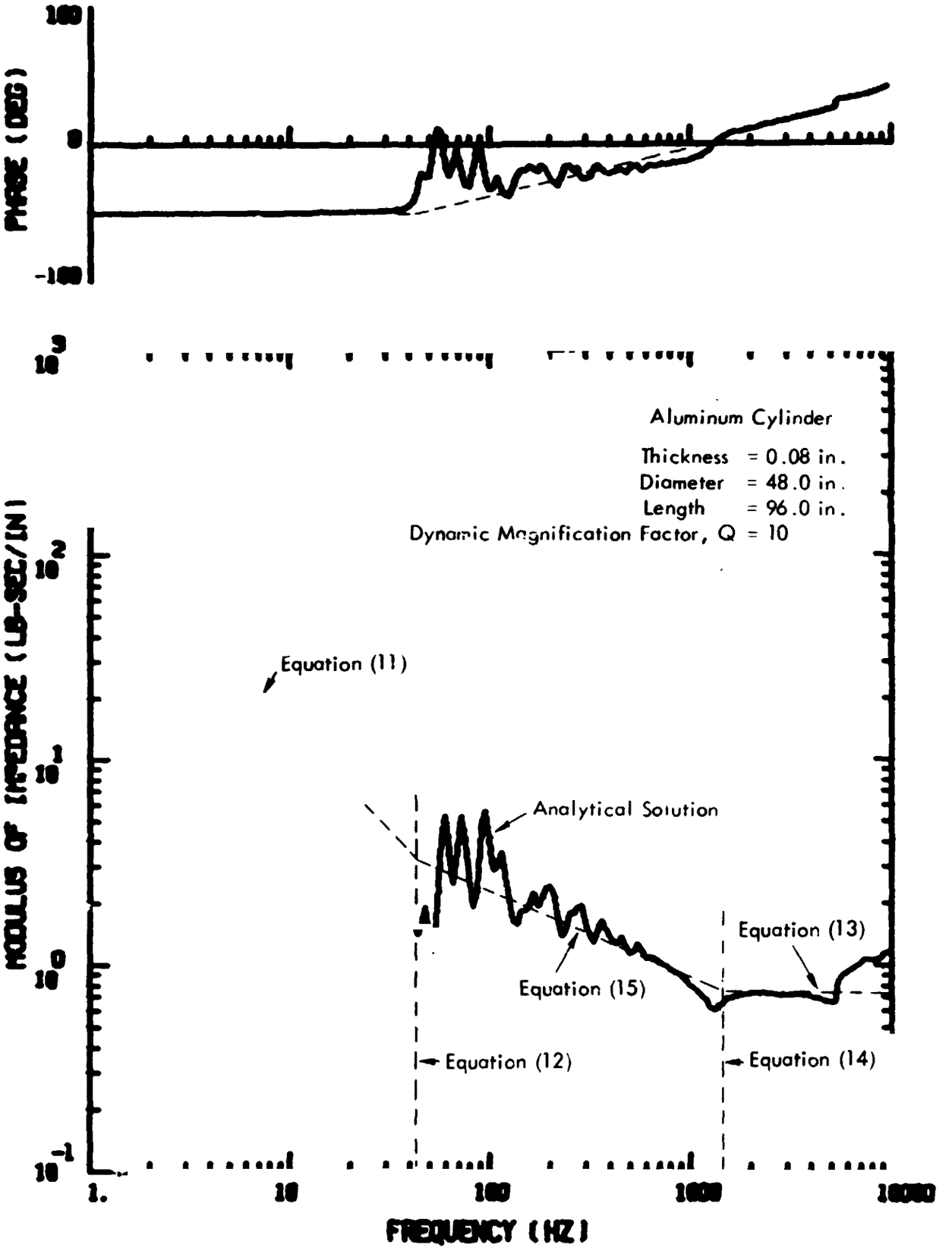

Figure C-3. Design Equations and Analytical Solution of Input Impedance at Mid-Length of an Unstiffened Cylinder

REFERENCES

1. Heckl, M.A., "Compendium of Impedance Formulas," BBN Report No. 774, May 1961.

2. Bozich, D.J. and White, R.W., "A Study of the Vibration Response of Shells and Plates to Fluctuating Pressure Environments," NASA CR-1515, March 1970.

3. Roark, R.J., "Formulas for Stress and Strain," McGraw-Hill Book Co., Fourth Edition, 1965.

4. Heckl, M.A., "Vibrations of Point-Driven Cylindrical Shells," JASA, Vol. 34, No. 10, October 1962.

5. Miller, D.K. and Harf, F.D., "Modal Density of Thin Circular Cylinders," NASA CR-897, December 1967.

6. Skudrzyk, E., "Simple and Complex Vibratory Systems," Pennsylvania State University Press, 1968.